Chapter 1

An overview of Energy, its various sources, and the key challenges associated with its storage and transformation

1.1 An introduction to energy

Energy is a fundamental characteristic of matter and space, playing a crucial role in every aspect of human life. From our daily interactions with the environment to large-scale industrialization, energy remains at the heart of all activities. Since the formation of planet Earth, energy exchange has been essential in making the planet habitable, making it a "foundation of existence" [1][2]. Millions of years ago, Homo sapiens came and slowly developed, especially during the Agricultural and Industrial Revolutions. Through time, humans learned to harness and use energy in all its forms to perform useful work. Although energy is broadly defined as the ability of a system to do work, its diverse forms make it difficult to provide a single definition that encapsulates all its forms. Nevertheless, energy is understood as a property of matter that can be transferred between systems but cannot be created or destroyed, forming the basis of the law of conservation of energy in physics.

As the standards of living and energy consumption rise exponentially, two trends are inescapable for the future: (1) the global population will continue to grow rapidly, and (2) reserves of fossil fuels such as oil, coal, and natural gas will decline significantly [3]. The world will face significant energy challenges and environmental concerns, including global warming and climate change, over the next few decades. These issues will need innovation technologies and lifestyle changes that could meet the increasing demands on energy while protecting environmental quality.

At present, the total number of people on Earth is about 8 billion, with an average of 3 MWh/year per capita of consumption. The energy coming from Earth's surface is primarily provided by the sun at 99.98%, a minute fraction from geothermal, and tidal/gravitational forces at 0.02%. Currently, the global energy consumption rate is about 17.4 TW which

accounts for only 0.008% of the solar energy hitting the planet—a number that is six times smaller than the energy absorbed through photosynthesis worldwide [4]–[6].

However, most of the solar energy hitting Earth depends on time, location, and weather conditions, making it not suitable for direct use in electrical and electronic applications. The additional challenges for renewable energy plants are that they are typically much smaller than the traditional power plants, and their output usually needs to be integrated into electrical grids to transport power to end users. Improving energy storage systems and conversion efficiency is thus essential to fully utilize renewable energy. Energy storage solutions at the grid scale are crucial to reduce reliance on fossil fuels and overcome the limitations of renewable energy sources.

1.2 Types of available Energy Sources

The Energy sources available globally can be broadly classified into two main categories: non-renewable and renewable energy sources.

1.2.1 Non-renewable energy sources

Non-renewable energy resources are those that cannot replenish themselves in a finite period. This makes their use unsustainable in the future. These include coal, oil, and natural gas which were formed millions of years ago through geological processes involving immense pressure and heat to break down ancient plants and animals into these energy sources. However, they are being consumed at a much greater rate than they can be replenished naturally, and that is going to eventually cause the exhaustion of these resources.

The extraction, processing, and burning of non-renewable energy sources also has severe environmental impacts. For example, burning fossil fuels emits tremendous amounts of

carbon dioxide (CO_2) and other greenhouse gases into the air. These lead to global climate changes because they trap heat from the environment and increase the Earth's temperature. The same elevated levels of CO_2 are also increasing air pollutants that pose severe health conditions for both human beings and the various ecosystems[7]. Moreover, extractions through mining and drilling often cause habitat destruction, leading to soil degradation and eventually water contamination, thus further negatively affecting the environment.

These negative effects have led most countries to work towards an alternative, away from using coal as a source of energy, and towards clean and sustainable sources. Renewable sources of energy, such as solar, wind, and hydroelectric power, are options that can be used for the supply of energy without further damage to the environment. These sources are replenished naturally in short periods and create little to no emissions; therefore, they are crucial to combating climate change and the sustainable use of energy in the future.

Here are some often accepted sources of non-renewable energies:

Figure 1.1: Different types of non-renewable energy sources [open access internet source]

1.2.2 Renewable energy sources

Renewable energy sources refer to resources that can regenerate themselves fast and consistently for a period of time so that their use is highly sustainable and reliable in meeting global energy requirements. Unlike the fossil fuel, which depletes after millions of years, renewable energy resources are always ready and are not depleted or exhausted while being used. These energy sources are considered pivotal for a future sustainable because these are abundant, non-polluting, and have reduced impacts on the environment compared with traditional energy sources.

This is the key reason; some of the most important merits of renewable energy are reducing emission of greenhouse gases and less air pollutants. Compared with fossil fuel combustion, emitting major amounts of carbon dioxide besides all known unhealthy pollutants like sulphur dioxide, renewable energy technologies operate rather clean with virtually no emission. This significantly helps fight climate change and reduce both air pollution and overall public health. Besides, renewable energy reduces reliance on fossil fuels associated with a plethora of environmental issues, such as oil spillage, habitat destruction, and resource depletion attributed to the extracting and transportation process[8]-[10].

Some of the most salient examples of renewable energies include:

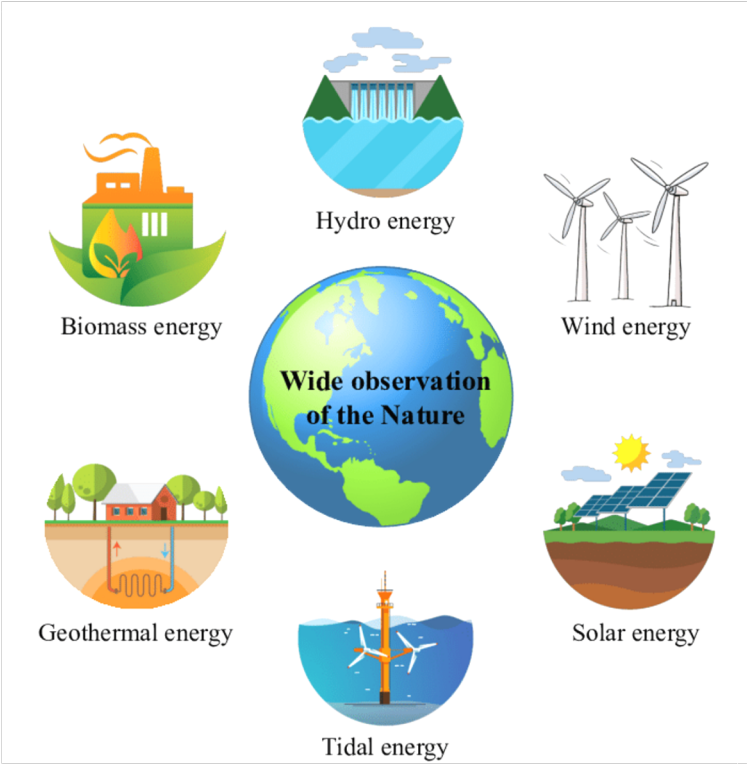

Figure 1.2: Different types renewable energy sources [open access internet source]

1.2.2.1 Hydropower or Hydroelectric Energy

Hydropower uses the energy of water as it moves from higher to lower elevations and can be produced either using reservoirs or rivers. Reservoir-based hydropower plants rely on stored water, whereas run-of-river plants capture energy from the natural flow of rivers. Hydropower reservoirs often serve multiple purposes, including providing drinking water, irrigation, flood and drought management, navigation, and electricity generation. Hydropower is also the largest source of renewable energy presently in the electricity sector. Again, however, it depends entirely on stable rainfall patterns - climate-induced droughts, or ecosystem changes that somehow alter precipitation, could be extremely challenging to overcome. Infrastructures needed for hydropower also tend to influence ecosystems negatively. Small scale hydropower is regarded as more environmentally friendly, but mostly for remote communities only [11].

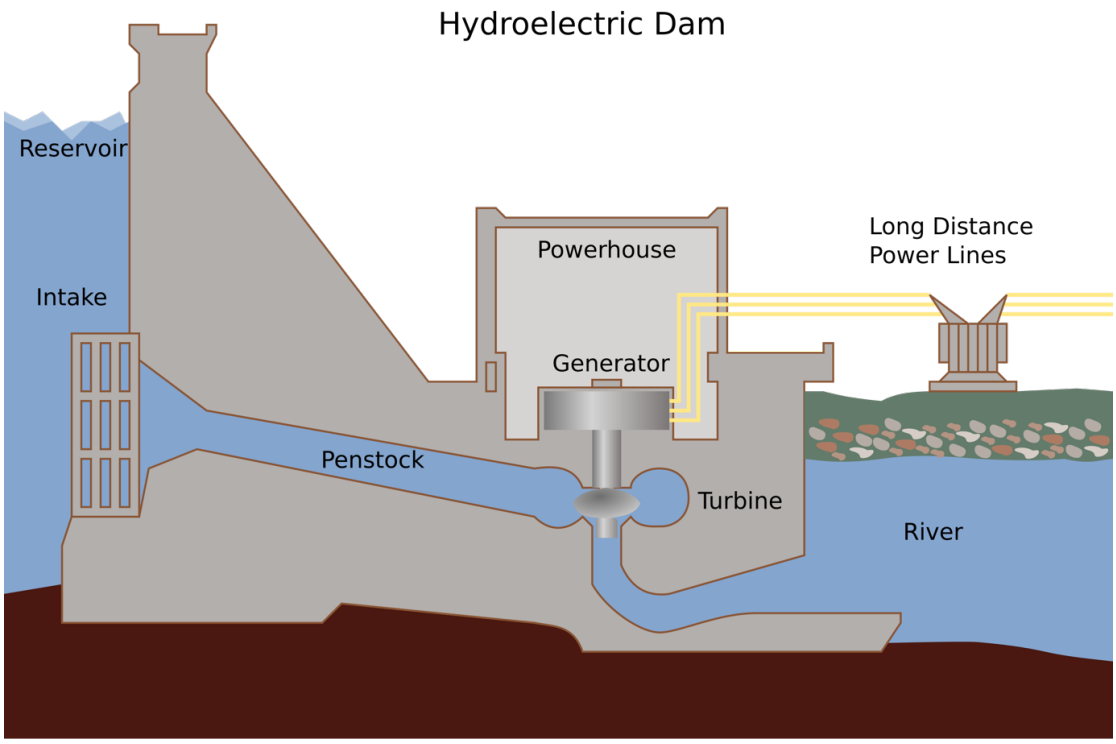

Figure 1.3: Hydrothermal energy[12] (Figure is taken from open access internet source)

1.2.2.2 Wind Energy

Wind energy utilizes the kinetic energy of moving air to generate electricity through huge wind turbines that can be placed on land or in bodies of water. Though humans have been harnessing wind energy for over a thousand years, new wind technologies both onshore and offshore within the last couple of years have been on increased production of electricity through higher turbines and larger rotor blades.

Although wind speed varies considerably with location, the overall potential for wind energy is many times larger than the electricity now being produced. Most regions of the world have sufficient wind resources to accommodate significant energy generation. However, the best wind conditions are generally located in remote areas. Offshore wind power presents great promise.[13]

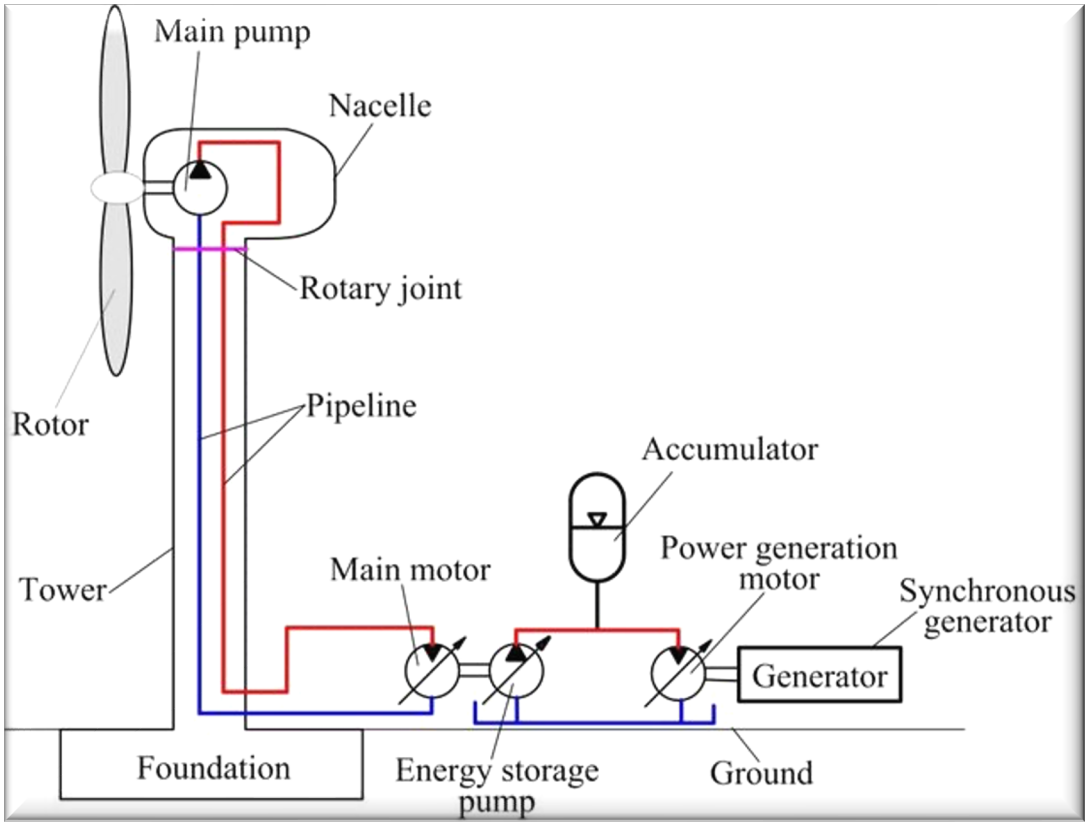

Figure:1.4: Wind energy [14]. (Figure is taken from open access internet source)

1.2.2.3 Solar Energy

Solar Energy is one of the most abundant energy resources, and it requires very little since it can be used even when cloudy. The total amount of solar energy reaching the earth is about 10,000 times larger than what humanity consumes altogether. This solar technology supplies heat and cooling, light, electrical power, and fuels for scores of applications. Solar technologies collect sunlight as electricity either via photovoltaic panels or mirrors that concentrate solar radiation. Despite its unavailability in some nations, every country can append a huge percentage to its share of energy. The cost to make the solar panels have fallen in the last decades making it not only accessible but, in many places, the cheapest way for generating electricity. On average, solar panels last for 30 years and comes in many shades depending on what is used in manufacturing it.[13]

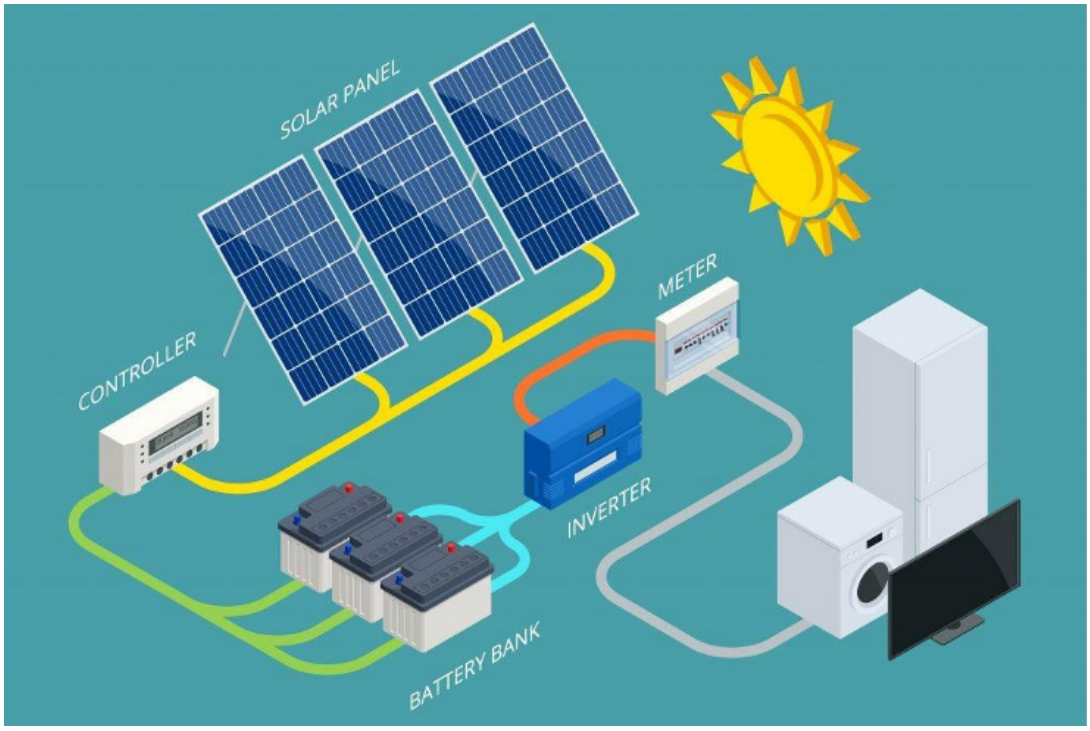

Figure 1.5: Solar energy [15]. (Figure is taken from open access internet source)

1.2.2.4 Ocean Tidal and Wave Energy

Ocean energy is generated from technologies capturing the kinetic and thermal potential of seawater, as in waves or currents. These systems are still at early stages of development, and wave and tidal current prototype systems are being tested. Theoretical potential for ocean energy is greatly in excess of the needs of the world today[13].

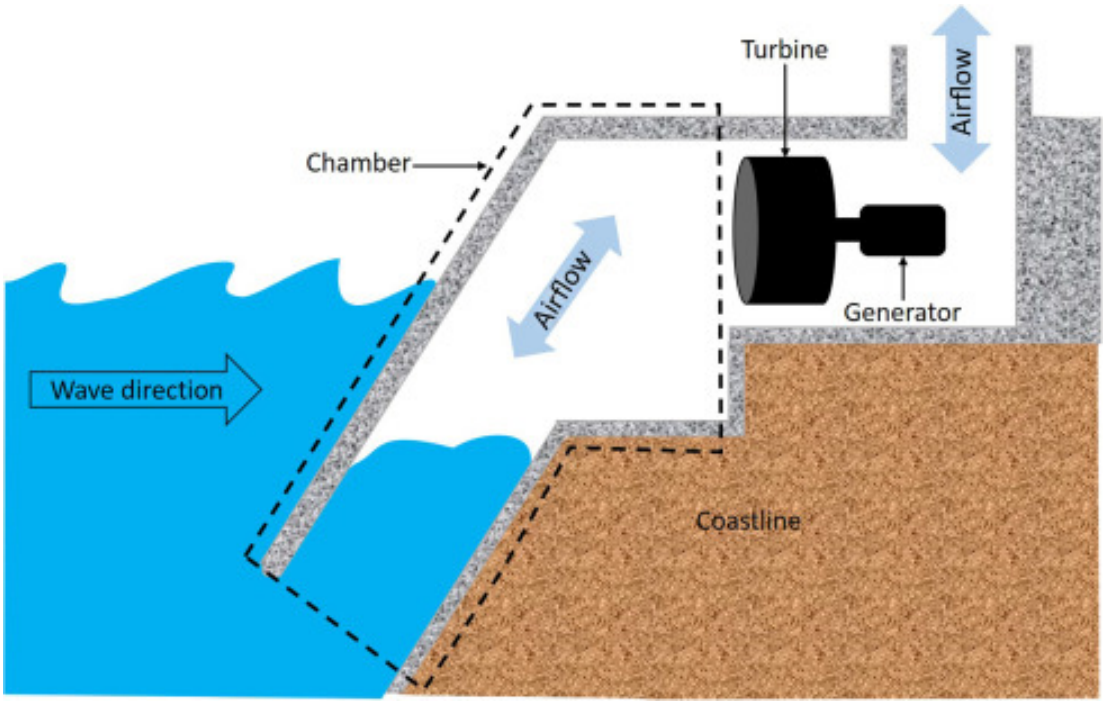

Figure 1.6: Ocean energy [18](Figure is taken from open access internet source)

1.2.2.5 Geothermal Energy

Geothermal energy is taken from the heat stored inside the Earth. This hotness is obtained from geothermal reservoirs through drilling holes or some other means of accessing them. Hydrothermal reservoirs are those that come naturally hot and permeable while those which need hydraulic stimulation to improve their permeability are known as enhanced geothermal systems. Fluid at various temperatures at the surface could be used to generate power. The technology of electricity production from hydrothermal reservoirs is well established, dependable, and in operation over one hundred years[13].

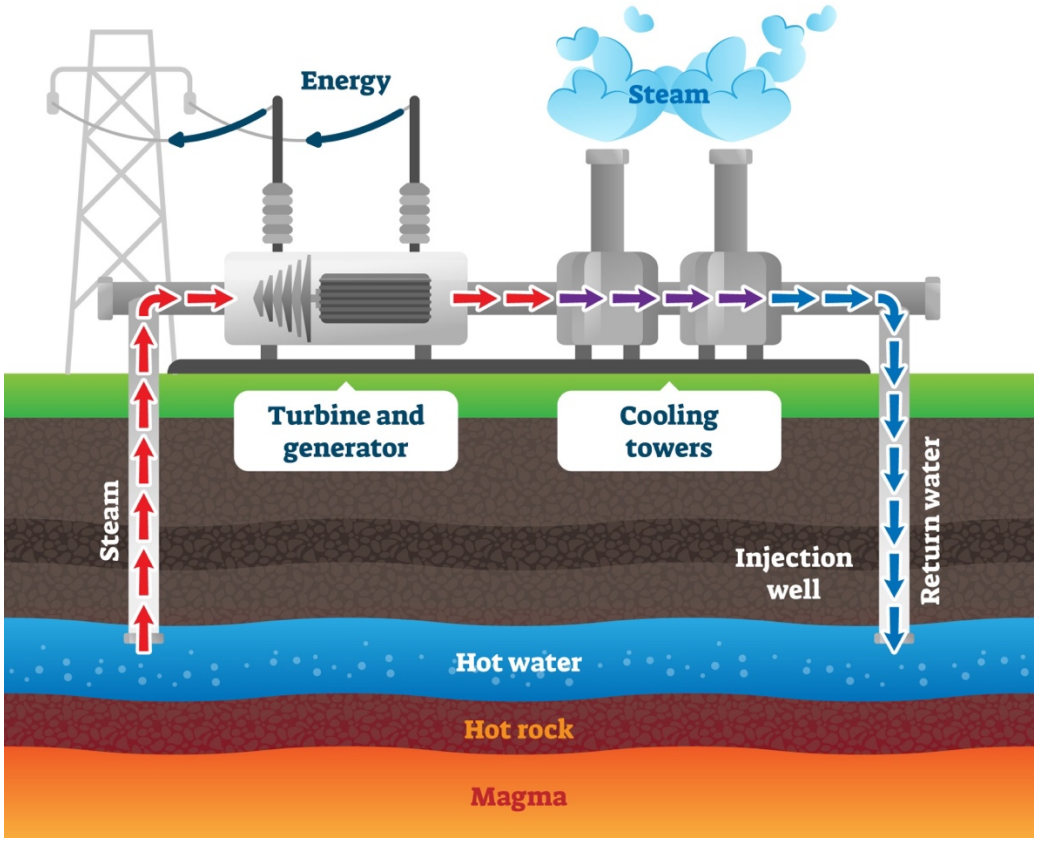

Figure: 1.7: Geothermal energy [17] (Figure is taken from open access internet source)

1.2.2.6 Bio or Biomass Energy

Bioenergy is produced from a wide variety of organic materials, known as biomass, such as wood, charcoal, animal dung, and other manures for heat and electricity, as well as crops for liquid biofuels. In the countryside, especially among the poor in developing countries, biomass is primarily used for cooking, lighting, and space heating. Dedicated crops or trees, agricultural and forestry residues, and other organic waste streams are also considered part of modern biomass systems. Although burning biomass results in the emission of greenhouse gases, the amount is usually smaller compared to fossil fuels such as coal, oil, or gas. However, it should be limited because there is potential negative environmental effect through large-scale bioenergy and forest plantations which can cause deforestation and land-use changes[13].

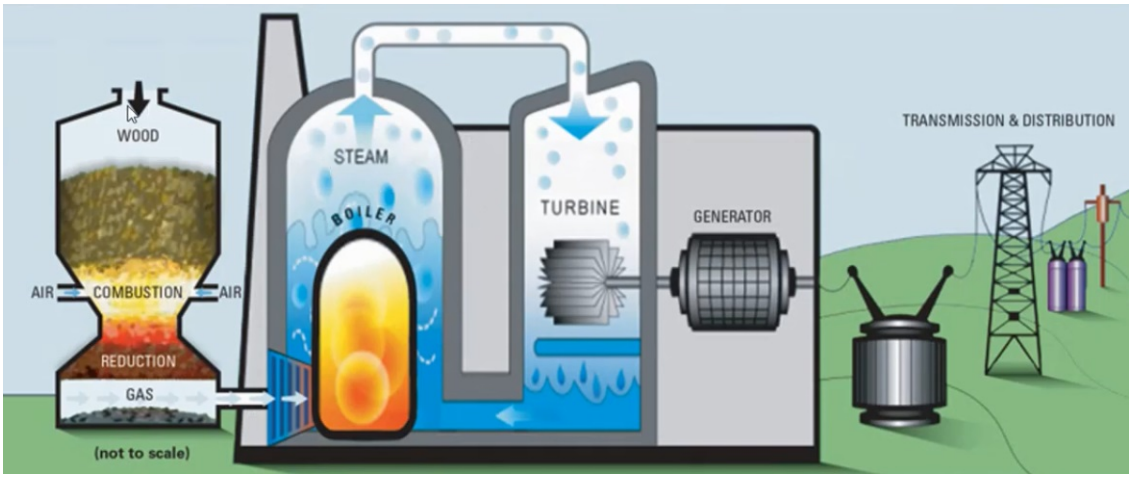

Figure 1.8: Bioenergy [18] (Figure is taken from open access internet source)

1.2.2.7 Problem associated with the renewable energy sources

A significant drawback which dilutes the benefits of these sources of renewable energy lies in their intermittency-the fact that they are generated partially unpredictably. More bluntly, it has proved difficult to integrate into an overall reliable power system an output which is intermittent to that extent [19]. Because the sources of renewable energy fluctuate in power as well as current due to factors unrelated to human control, such as varying intensity of solar incidence and changing wind velocities during changes in weather conditions at any time, the supply would not match the demand anywhere at all times, or vice versa. It requires a viable energy storage technology in the field of renewable energy [20].

1.3 Necessity of renewable energy sources and its challenges

Most significantly, one of the major motives in embracing renewable energy sources is to reduce reliance on fossil fuels and alleviate environmental degradation through global warming and climatic change [21][22]. It uses all those technologies that give an effective renewable alternative to lower greenhouse emissions to a great extent and significantly decrease air pollution. For an effective response to the climate change issue, renewable energy technologies will have to emit virtually no or very little CO_2 into the atmosphere.

Improving energy security by reducing imports of foreign energy supplies is one of the other key priorities. Since renewable resources are abundant in the domestic territory, renewable energy can be produced close to the user, making it less exposed to geopolitics and price volatility inherent in fuel imports. As a result, renewable energy sources support a sustainable and resilient energy future through the reduction of greenhouse gas emissions, fight against climate change, and provision of stable, affordable energy supply in the world.

Despite their potential, most renewable energy technologies are still in their developing stage. The supply of renewable energies is unreliable and changes over time and weather conditions. Energy generated from solar and wind is dependent on sun shine and wind speed respectively. Intermittence poses complexity in grid stability, which is why the balancing needs of fluctuating supply and demand call for the presence of energy storage systems and smart grid technologies [23]. The existing grids that have been designed for centralized fossil fuel-based power need to be transformed to accommodate the spread of renewable energy sources. Besides this, upgrading and expansion of transmission and distribution infrastructure so as to connect renewable generation sites to urban centers have challenges related to logistics and financial requirements. Thus, maintaining an even balance between energy supply and demand calls for developing smart energy storage solutions [24]. These challenges can be met through continuous research, technological innovation, supportive policies, and international cooperation to accelerate the transition towards a sustainable energy future.

1.4 Renewable Energy storage solutions

Renewable energy storage solution systems refer to the technologies which can store energy generated from renewable sourced from solar, wind, hydro, or geothermal powers. The technologies are integral parts for rebalancing the demand for energy and supply by stabilization in the grid and integrating into a power network the energy sources. There are currently plenty of storage solutions out there which are used daily, with examples as listed below:

1.4.1 Mechanical energy storage

The flywheel energy storage system (FESS) is the mechanical storage device that reproduces electrical energy storage as it transforms the energy to kinetic form which is further stored in a rotating mass with minimal frictional losses [25]. Energy inputs to the FESS come from the electrical source available from the grid or from any other electrical energy. An integral motor generator is accelerating with storing of the energy and retards the motion of its discharge.

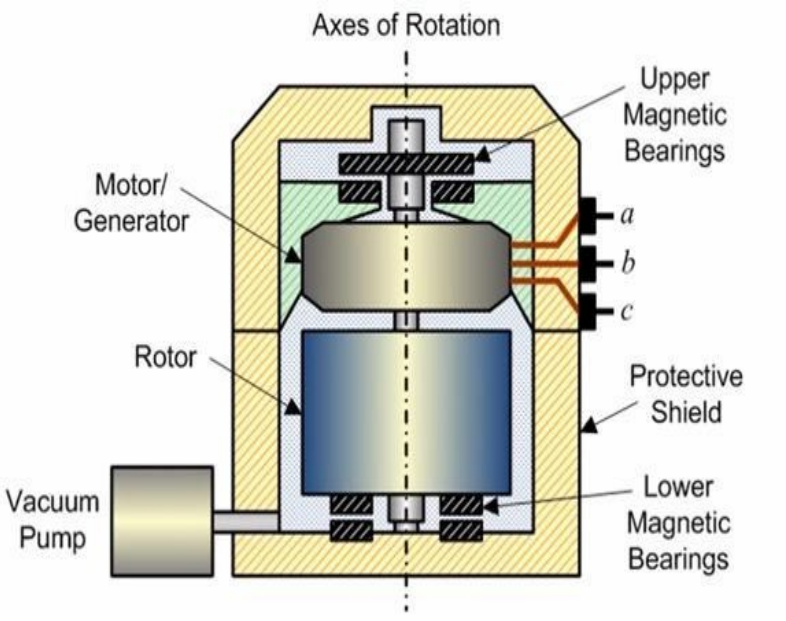

Figure 1.9: Mechanical energy by a flywheel [26] (Figure is taken from open access internet source)

1.4.2 Thermal energy storage

Thermal energy storage (TES) spans a range of technologies that can store thermal energy in all three forms: sensible heat, latent heat, and even chemical energy in the context of thermochemical reactions.[27] Of these, sensible heat storage stores energy based on the material's specific heat capacity and is stored in tanks that are quite thermally insulated.[28]

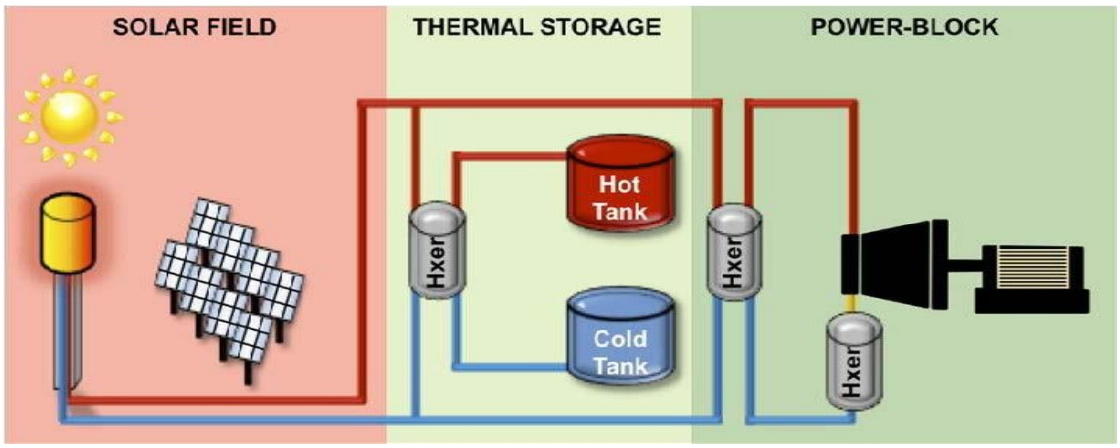

Figure 1.10: Sensible heat energy storage system [29] (Figure is taken from open access internet source)

1.4.3 Superconducting Magnetic Energy Storage (SMES)

The system consists of three components: the coil, PCS, and a cooling system. The basis of the concept is that a current will continue to flow through a superconductor even after the voltage supply is cut off. The resistance of the superconductor coil goes nearly to zero, so even when the voltage source is disconnected, the current continues to flow in the coil.[30][31] Energy is stored as a magnetic field produced by the current in the superconducting coil, and this energy can be released by discharging the coil.

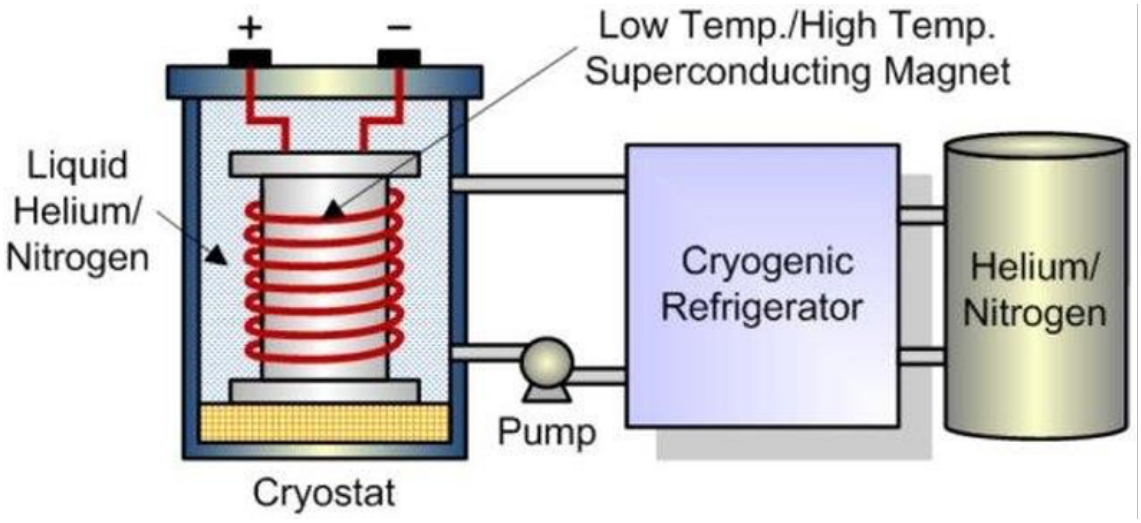

Figure 1.11: Superconducting Magnetic Energy Storage (SMES) component system [32]. (Figure is taken from open access internet source)

1.4.4 Hydrogen Energy Storage

Water electrolysis technology provides the most flexible and sustainable means of storing renewable energy on a large, long-term scale. Using surplus renewable electricity, the PEM splits water into its constituent parts: hydrogen and oxygen, which can then be stored in standard tank.[33][34]

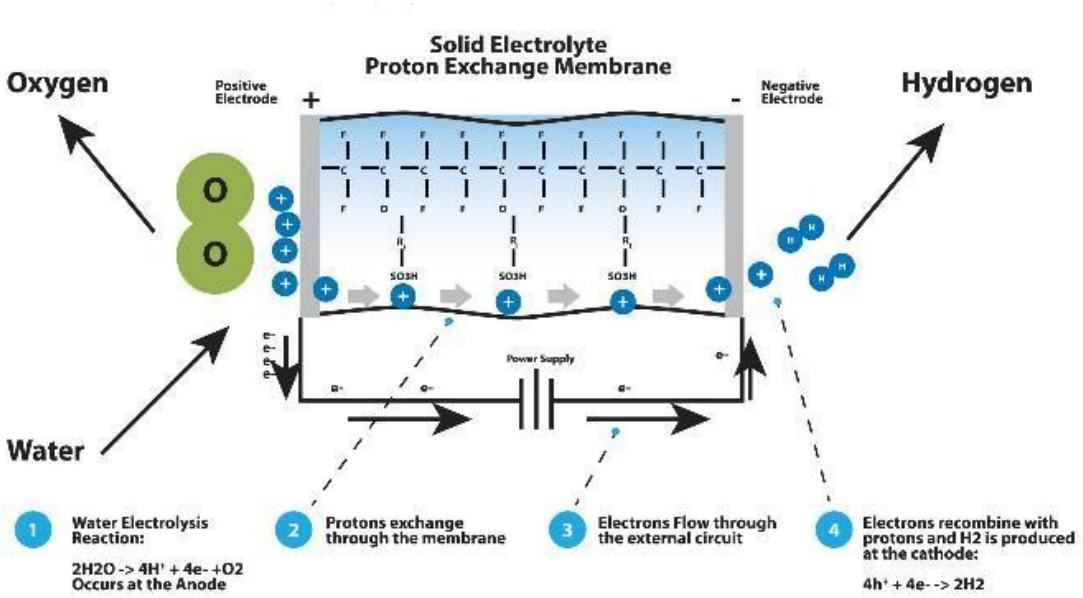

Figure 1.12: Chemical process of hydrogen production [35]. (Figure is taken from open access internet source)

1.4.5 Electrochemical Energy Storage (EES) Systems

Electrochemical energy storage devices have received a significant amount of attention in the recent past due to the high conversion efficiency and swift power delivery. These store energy in the form of a chemical reaction and deliver it through electrical energy when needed. The ever-increasing use of mobile devices, electrical vehicles, and the Internet of Things have increased the research in finding more efficient EES.[36]-[39] Essentially, all such devices depend on the movement of ions between two electrodes, with the flow of electrons in an external circuit[40][41]. Ideally, an EES device should be able to store a large amount of energy (high specific energy) while also supporting rapid charging and discharging (high specific power), as in a Ragone plot[39][42], which depicts the relationship between the energy density of different devices measured in Wh/kg and power density in W/kg. Among the available EES options, fuel cells have the advantage of possessing a very high energy density, but this comes with low kinetics slow power density and expensive catalysts. Capacitors suffer from an energy density that is so low they are used for slow-power applications and nothing faster than that.

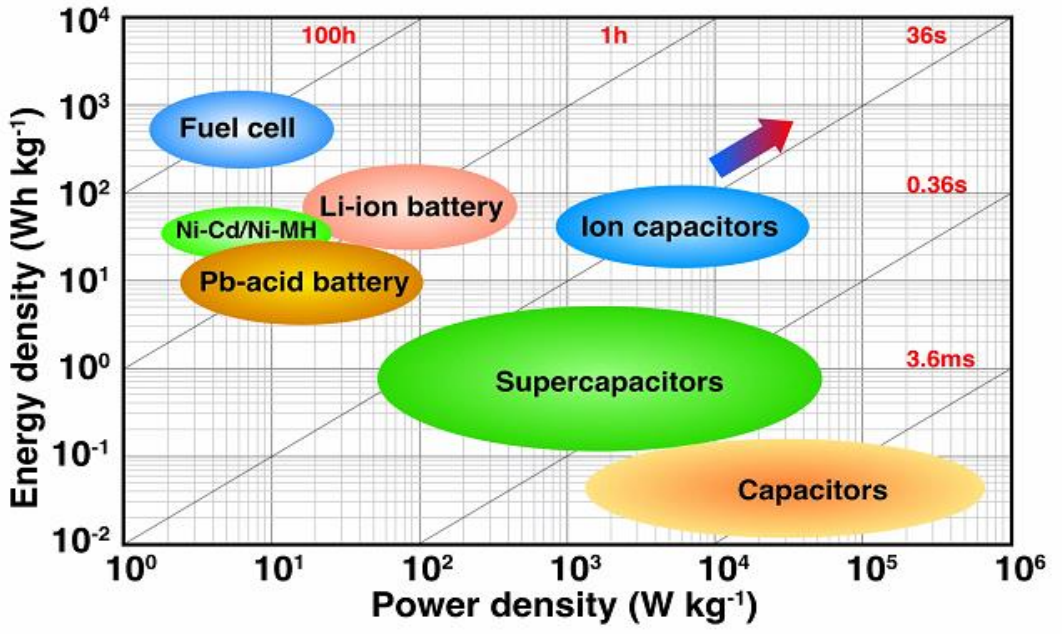

Figure 1.13: Rangone plot demonstrating energy and power relationship of different EES system [42]

As a result, the batteries as well as Supercapacitors have emerged as primary energy storage technologies in the market. More recently, a series of extensive research initiatives are aimed towards improving metal-air batteries, lithium/sodium-ion batteries as well as Hybrid and Asymmetrical Supercapacitor with pseudocapacitive electrodes, both of which are expected to meet near-future large-scale energy storage together with rapid power requirements.

1.4.6 Historical Perspective

Electrochemistry was studied and discovered by the late 18th century, when Luigi Galvani noted that a frog's leg twitched on contact with a charged metal scalpel. Alessandro Volta developed the first battery called the Voltaic pile, shown in **Figure 1.14**, after this pioneering observation. The Voltaic pile was an arrangement of copper and zinc disks alternating between each other with cardboard pieces soaked in saltwater between them. This invention served as the stepping stone towards the discovery of water electrolysis and establishment of various laws of electrochemistry.

Figure 1.14: voltaic pile [43] (Figure is taken from open access internet source)

Interestingly, most battery technologies being used or developed today originated in the past two centuries, with the lithium-ion battery being the only exception.

Table 1.1 Development of various battery technologies [44]

Inventor	Technology	Year
A. Volta	First battery	1800
J. Frederic Daniell	Zn-Cu battery	1836
A. Smee	Metal air batteries	1840
G. Plante	Lead-acid battery	1859
G. Leclanché	Zn MnO_2 Battery	1868
T. deMichalowski	Ni-Zn battery	1899
W. Jungner	Ni-Cd battery	1901
Multiple inventors	Li-ion battery	1991

The first capacitor was named the "Leyden jar" and was invented by Ewald Georg von Kleist and Pieter van Musschenbroek in the mid-18th century [45]. EDLCs were first explained in the 19th century, with the support of interfacial electrochemists like Gouy [46], Chapman [47], Stern [48], and Grahame [49]. A new class of electrochemical capacitors was discovered in 1971, termed pseudocapacitors, these involved Faradaic processes, especially in RuO_2.[50][51] Pseudocapacitance marked the first major step forward toward an enhancement of energy densities for electrochemical capacitors.

1.4.7 Electrostatic Capacitors

There are three main classes of electrostatic capacitors: conventional capacitors, electrolytic capacitors, and ceramic capacitors. While conventional capacitors consist of two metallic electrodes separated by a dielectric material, the electrolytic capacitors use an electrolyte to act as a conductor between the dielectric and one electrode and have the working voltage dictated by the thickness of the dielectric. Ceramic capacitors are formed by an alternate layering of metals and ceramics, with the ceramic acting as the dielectric.[52] The charge storage capacity is determined by Eq. 1.1.

$$Q = CV \tag{1.1}$$

where Q represents the stored charge, V is the voltage between the plates, and C is the capacitance [53]. For an electrostatic capacitor, its capacitance is governed by Eq. 1.2.

$$C = \varepsilon 0 \varepsilon r \frac{A}{d} \tag{1.2}$$

The total energy and maximum power stored in a capacitor are given by Eq. 1.3 and Eq. 1.4

$$E_{Total} = C \int_{V_{min}}^{V_{max}} V \, dV = \frac{1}{2} CV^2 \tag{1.3}$$

$$P = IV = \frac{V^2}{4R_{cap}} \tag{1.4}$$

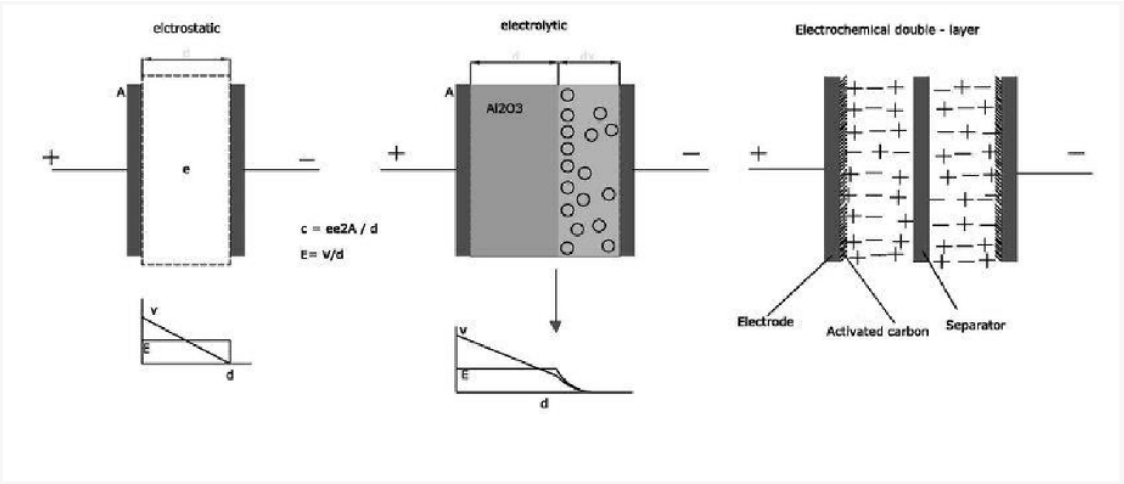

Figure 1.15: Schematic presentation of the electrostatic capacitor, electrolytic capacitor, and electrical double layer capacitor[52]

1.4.8 Batteries

A battery is a device that stores energy by forming chemical bonds and converts it into electrical energy through an electrochemical redox reaction. The total stored energy (G) in a battery depends on the overall capacity (Q) and the voltage (V), expressed as an integral function.

$$G = \int Q \, dV \qquad (1.5)$$

The relationship between capacity and voltage is quite different for various battery materials due to the unique characteristics of their faradaic reactions. These reactions often involve phase changes as the electrode material undergoes oxidation or reduction.

$$O + ne^- \leftrightarrow R \qquad (1.6)$$

Equation (1.7) derived from equation (1.5) for an ideal battery with a voltage (V), the total stored energy (G) is simply:

$$G = QV \qquad (1.7)$$

The theoretical (or maximum) capacity of a battery material can be determined by knowing the redox reaction taking place and by using Faraday's laws of electrolysis which state that:

$$Q = \frac{nF}{M} \qquad (1.8)$$

Where F is the Faraday constant (96485 C mol^{-1}), n is the number of electrons transferred, and M is the molar mass of the material. The potential of a battery material (E^0) is directly related to the change in the Gibbs free energy (ΔG) of the reaction and thus chemical potential (Δμ) upon reduction [54]:

$$E^0 = -\frac{\Delta G}{nF} = -\frac{\Delta \mu}{nF} \qquad (1.9)$$

This relationship forms the basis of the Nernst equation, which also accounts for the different activities of the materials involved in the redox reaction.

Furthermore, Batteries can broadly be categorized into two types: primary and secondary batteries. Primary batteries are used once and then disposed of when they are fully depleted. While Secondary batteries, also known as rechargeable batteries, can be recharged and reused several times before being discarded. Examples of secondary batteries include lithium-ion, nickel-cadmium, and lead-acid batteries.

1.5 Types of rechargeable energy storage devices

Secondary batteries could be broadly classified into two types depending on their chemical composition and electrolyte layout: aqueous electrolyte based and non-aqueous electrolyte based. Aqueous electrolyte-based batteries include the lead-acid battery, nickel-cadmium, nickel-metal hydride, flow batteries, metal-air, etc. But non-aqueous-based electrolyte batteries include a lithium-ion battery, Lithium polymer battery, or sodium-ion battery.

1.5.1 Lead-acid battery

The lead-acid battery offers several advantages over other electrochemical energy sources. The cost is relatively low and lead is abundant, which means that performance is reliable, the cell voltage is high at 2 V, electrochemical efficiency is good, and the cycle life varies from a few hundred to thousands of cycles. These attributes make lead-acid batteries suitable for medium to large-scale energy storage applications since they provide a balanced mix of power capabilities and affordability. They usually consist of multiple cells connected in series. The essential components of a lead-acid battery include electrodes, separators, electrolytes, containers with lids, ventilation systems, and other auxiliary parts.[55]

The active material of a lead-acid battery is applied in the form of lead oxide (PbO) to a grid, which electrochemically transforms into reddish-brown lead dioxide (PbO_2) on the positive electrode and gray spongy lead (Pb) on the negative electrode. Separators are used to electrically isolate the positive and negative electrodes, and an aqueous sulfuric acid (H_2SO_4) solution with a density in the range of 1.22 to 1.28 g/cm³ acts as the electrolyte.[56]

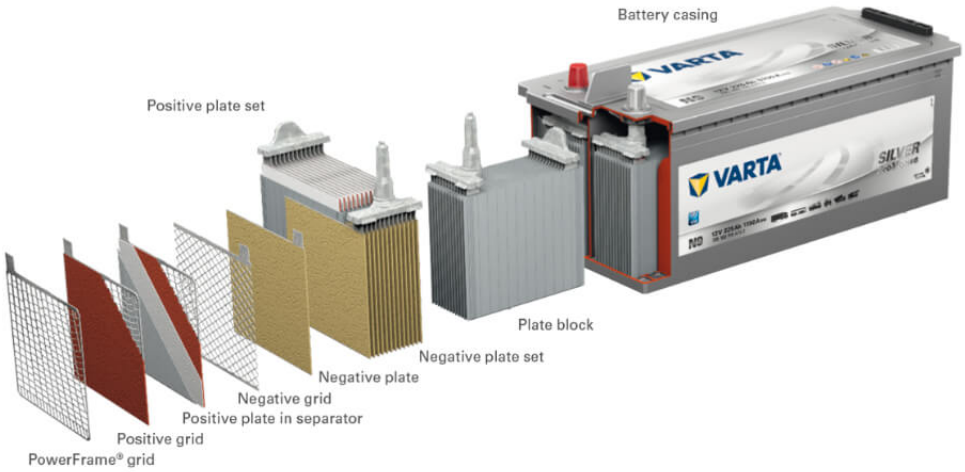

Figure 1.16: Lead acid battery [57] (Figure is taken from open access internet source)

Overall discharge reaction of Lead acid battery:

$$PbO_2(s) + Pb(s) + 2H_2SO_4(aq.) \rightarrow 2PbSO_4(s) + 2H_2O \qquad E^0 = +2.048\ V \quad (1.10)$$

The lead-acid battery is widely used for starting automobile internal combustion engines and for the power supply of electrical devices when the engine is turned off. It is also used as a power source for industrial trucks, delivery vehicles, and as stationary batteries to ensure an uninterrupted power supply in case of grid failures. The battery usually lasts for about 5 years or 1,000 charge-discharge cycles.

However, lead-acid batteries have problems such as positive plates expansion, water loss from gassing or high temperature, acid stratification, positive grid corrosion, and sulphation of active material because the battery is not fully charged. These are major problems if the battery is to work in a partial state of charge as in the Hybrid electric vehicle and remote area power supply systems.[58]

1.5.2 Lithium-ion battery

Lithium-ion batteries have been the key to portable electronics for the last 30 years. These batteries store energy through the reversible insertion of lithium ions into both the cathode and anode. While the process of lithium insertion into transition metal compounds was discovered in the 1970s[56], it was only with the development of lithiated transition metal oxides and lithium intercalation into graphite that Sony was able to commercialize the first battery. A standard lithium-ion battery, as shown in **Figure 1.17**, typically uses $LiCoO_2$ for the cathode and graphite for the anode. This configuration gives a very high cell voltage of about 3.6 V and an energy density in the range of about 120-150 Wh kg^{-1}.[59] The electrolyte is a mixture of organic solvents like ethylene carbonate and dimethyl carbonate containing $LiPF_6$ dissolved in it.

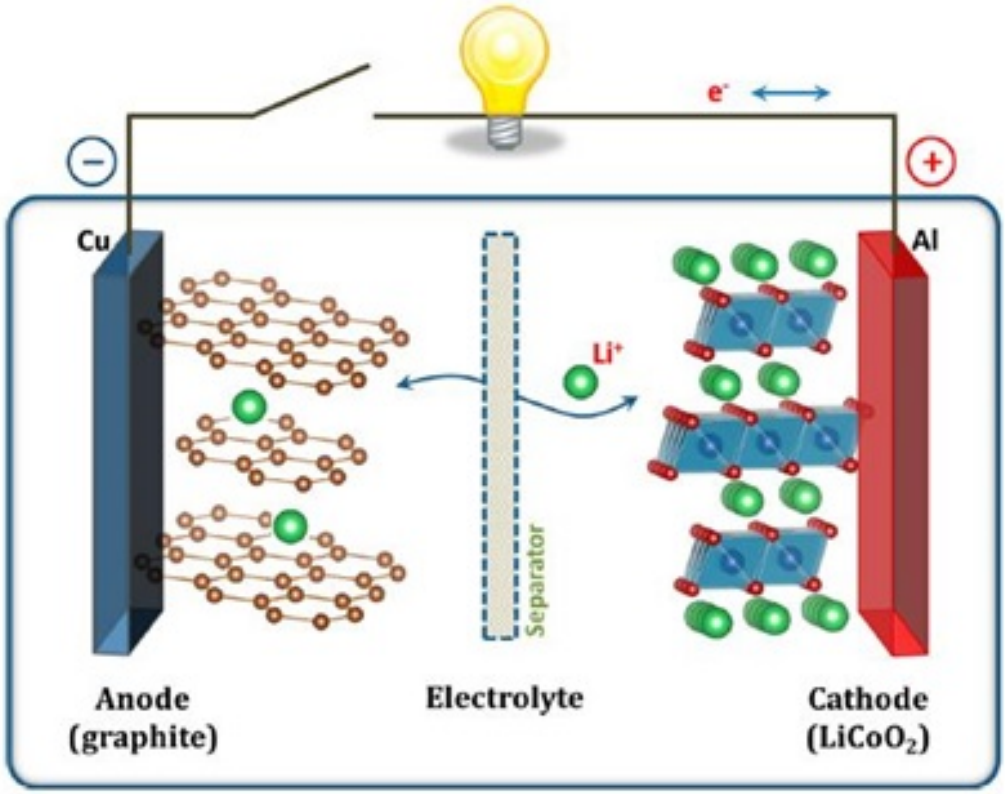

Figure 1.17: Configuration of Li-ion Battery[56]

The reactions during the energy-storage (charging) stage are:

Reaction on Cathodic electrode:

$$LiCoO_2 \leftrightarrow Li_{1-x}\, CoO_2 + xLi+ + xe^- \quad (1.11)$$

Reaction on Anodic electrode :

$$C_6 + Li+ + e^- \leftrightarrow LiC_6 \quad (1.12)$$

Intercalation reactions can offer high reversibility since the voltage differences in the insertion and removal process are low for many materials, a commercial lithium-ion batteries can be rated up to 500 charge/discharge cycles[60]. However, when these materials exceed their stability limits, they undergo massive structural changes and dissolution, causing problems such as capacity degradation and thermal runaway. Intercalation reactions store one lithium ion per formula unit and despite the extensive research on this subject, this number has not increased over time. To improve the energy density, the voltage of the cathode material may be elevated above the 3.6-3.9 V range of $LiCoO_2$ because the voltage of graphite is rather low. A few high-voltage cathodes have been proposed. One family of such materials involves the spinel structure $Li_yM_xMn_{2-x}O_4$ where M can be Cr, Fe, Co, Ni, or Cu.[61] These materials have energy storage between 4 and 5 V. However, in this approach, there is a problem of finding suitable electrolytes for a 5 V potential window.

1.5.3 Challenges and shortcomings of Li-ion batteries

Despite their technological potential, Li-ion batteries are still plagued by several issues, mainly on the safety side. They are sensitive to high voltages and tend to overheat and get damaged. At times, this may trigger thermal runaway and fires[62]. Moreover, Li-ion batteries deteriorate with time, resulting in loss of capacity and frequent failures within a few years of operation.

Another drawback for their widespread use is the relatively high cost-about 40% more expensive-than batteries. In addition, these cells are not designed to support fast charge storage as is needed for such applications as regenerative braking.[63]

Although significant improvement of the past years has been there in improving the performance of batteries, main concerns remain with peak usage[64]. Batteries can get ruined by a sudden energy request in even small devices, such as mobile phones or laptops. The issue grows in importance in EV, as variables like driving patterns and road conditions result in fast variations in power demands. The best operation of the batteries happens when they are discharged in a steady rate as the electrochemical reaction proceeds smoothly. However, in cases where the EV needs sudden power to accelerate, the battery cannot deliver power fast enough to the vehicle. The same problem is experienced during braking where high electric currents that go in and out of the battery cause it damage due to electrolytes. The repeated acceleration and braking in city driving reduce the battery life. Thus, there is a need for an alternative solution to the problems of limited lifespan of the battery and insufficient power output. The current demand is for devices that combine high power, energy density, and long cycle life.[65] Modern high-power applications require large amounts of energy delivered quickly, which batteries and capacitors alone cannot provide.[66] To address these requirements, Supercapacitors have been designed within the last few decades as an answer to conventional energy storage problems.

1.5.4 Supercapacitors

Supercapacitors also known as ultracapacitors are advanced energy storage equipment that offers a balanced blend of power and energy performances. They have many benefits, including being able to be charged/discharged rapidly and very long cycle life, making Supercapacitors ideal for power-intensive applications. Currently, Supercapacitors are used in addition to the

battery in electric vehicles, with them reducing the overall power source size, enhancing battery life, and minimizing energy losses.[67] The difference between the conventional capacitors and the Supercapacitors is that the Supercapacitors have both electrostatic double-layer capacitance and electrochemical pseudocapacitance. Energy storage devices (ESs) can be classified into two types based on the charge storage mechanism[68]: (i) electrochemical double-layer capacitors (EDLCs) and (ii) pseudocapacitors.

1.5.5 Electrochemical double-layer Capacitors (EDLC)

In EDLCs, the charge-discharge process is based on the accumulation and separation of electrostatic charges at the electrode/electrolyte interface on both electrodes, as depicted in **Figure 1.18**. The capacitance resulting from this interface is known as double-layer capacitance (C_{dl}). [69] Similar to conventional capacitors, EDLCs possess positive and negative electrodes submerged in an electrolyte; however, they offer much greater capacitance per volume by employing high-surface-area porous carbon materials as the active components.

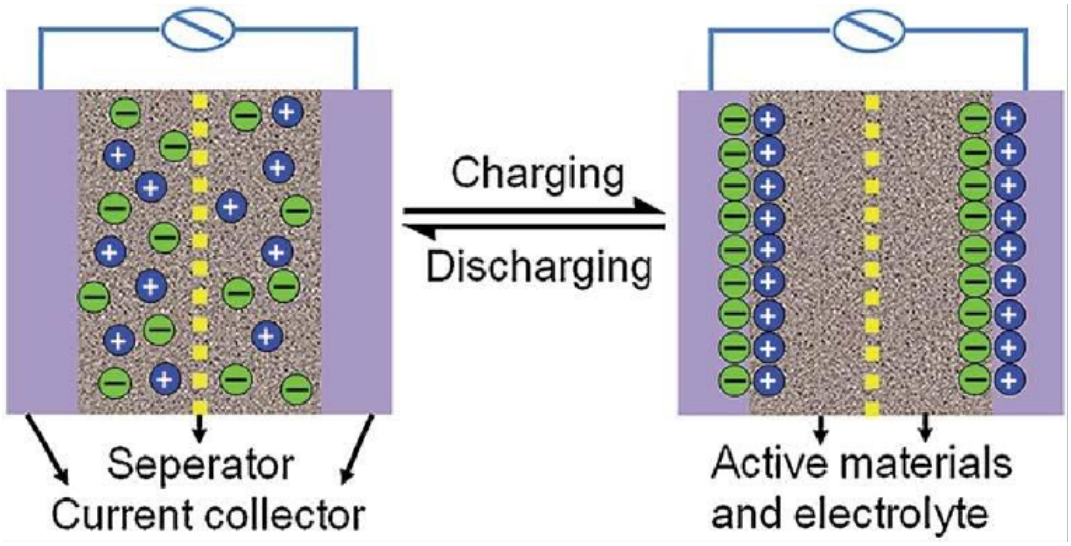

Figure 1.18: Charge storage mechanism of EDLC [70]

1.5.6 Charge Storage mechanism in EDLC

The mechanism of charge storage involves an explanation of the origin and models of the double-layer concept. Double-layer theory was originally conceived by von Helmholtz. In this model, there exist two layers of opposite charges which are separated by atomic distances that are very small. The Helmholtz model is shown in **figure 1.19(a)** where a compact static array of ions surrounds the charged electrode surface. Later, Gouy and Chapman developed an improved version of the Helmholtz model that takes into account the influence of thermal fluctuations on the ions in the electrolyte following the Boltzmann principle. In their improved model **(Figure 1.19(b)**, Gouy and Chapman treated ions as point charges and incorporated these thermal effects. However, the assumption of point charge ions resulted in the weaknesses and failure of the Gouy-Chapman model, which clearly showed that the more accurate representation of the interactions between ions at the electrode/electrolyte interface was required.

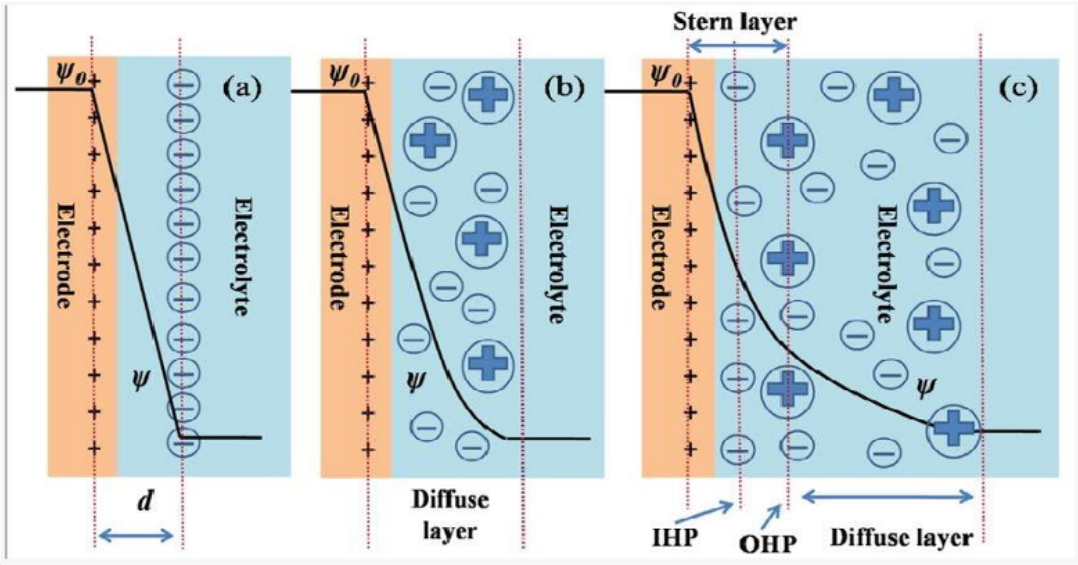

Figure 1.19: (a) Helmholtz model, (b) Gouy-Chapman model, and (c) Stern Model [71] (Figure is taken from open access internet source)

The Stern model (**figure 1.19 (c)**)is able to provide a more detailed description of the double-layer phenomenon than both the Helmholtz and Gouy-Chapman models. Equation 1.13 relates

the electrode's double layer capacitance C_{dl} to the contributions of both the Helmholtz C_H and diffuse layers C_{diff} and the corresponding equivalent circuit diagram:

Figure 1.20 Stern model circuit diagram for double layer capacitance (C_{dl}) (Figure is taken from open access internet source)

$$\frac{1}{C_d} = \frac{1}{C_H} + \frac{1}{C_{diff.}} \qquad (1.13)$$

Grahame modified the Stern model by including ionic radii and the polarizability of the cations and anions present in the electrolyte solutions. [71] An important feature of the Grahame model is that the closest approach distances between cations and anions toward the electrode surface have to be distinguished. In particular, because of a solvation shell around cations, they are located further away from the electrode surface than anions. [71] This distance difference gives rise to the splitting of the Helmholtz layer into inner and outer Helmholtz layers, as illustrated in **Figure 1.21**. Hence, Eq. 1.13 can be written as Eq. 1.14 with the contributions of capacitance due to the inner (C_{IH}) and outer (C_{OH}) Helmholtz layers:.

$$\frac{1}{C_{dl}} = \frac{1}{C_{IH}} + \frac{1}{C_{OH}} + \frac{1}{C_{diff.}} \qquad (1.14)$$

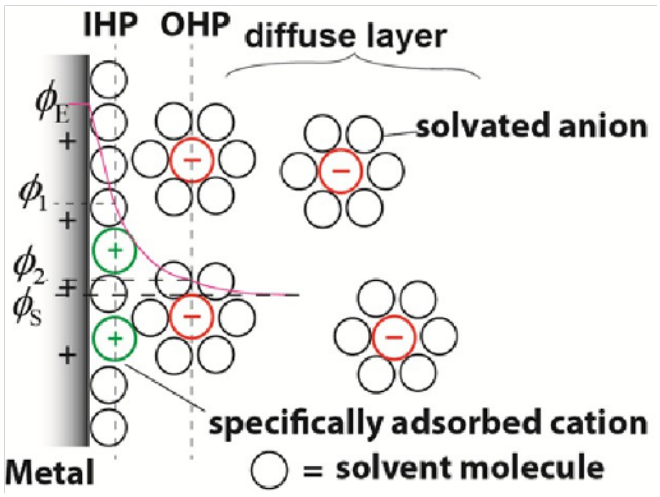

Figure 1.21: Representation of Grahame model [72] (Figure is taken from open access internet source)

In commercial EDLCs, porous carbon materials are frequently used as the active components and have surface areas in a range of 500 to 3000 m^2/g.[74] This research has indicated that electrodes based on carbon possess capacitance density, C_{dl}, between 15 and 50 $\mu F/cm^2$ in aqueous electrolytes.[75] Using an average C_{dl} value of 30 $\mu F/cm^2$ and a surface area of 1000 m^2/g, the theoretical capacitance of such carbon materials comes out to be 300 F/g. However, actual capacitance achieved can go below 50 F/g because of limited electrolyte access to the pores and low electrical conductivity.[76]-[78] With the smaller capacitance, however, EDLCs act completely electrostatically with no phase change, so that they are able to possess an extremely long cycle life. The voltage window for aqueous EDLCs is usually limited to about 1.4 V to avoid water decomposition, whereas with organic electrolytes, EDLCs can be operated up to 3.5 to 4 V.[75] Although EDLCs with organic electrolytes have higher energy density, they suffer from higher electrolyte resistance, which reduces their power density.

1.5.7 Pseudocapacitors

In pseudocapacitors, the energy is stored by a fast and reversible redox reaction that takes place at the surface of the electrode. This is different from EDLCs because pseudocapacitors provide 10 to 100 times more capacitance since the storage is not only at the surface but also in the vicinity where the diffusion of ions happens.[79] The faradic process is slower, however, which decreases the power of the pseudocapacitor compared to EDLC. In pseudocapacitance, the potential of the electrode is logarithmically proportional to the extent of the reactions. Conway identified three faradic systems capable of generating pseudocapacitance: (a) underpotential deposition, (b) redox pseudocapacitance, and (c) intercalation pseudocapacitance.[80]

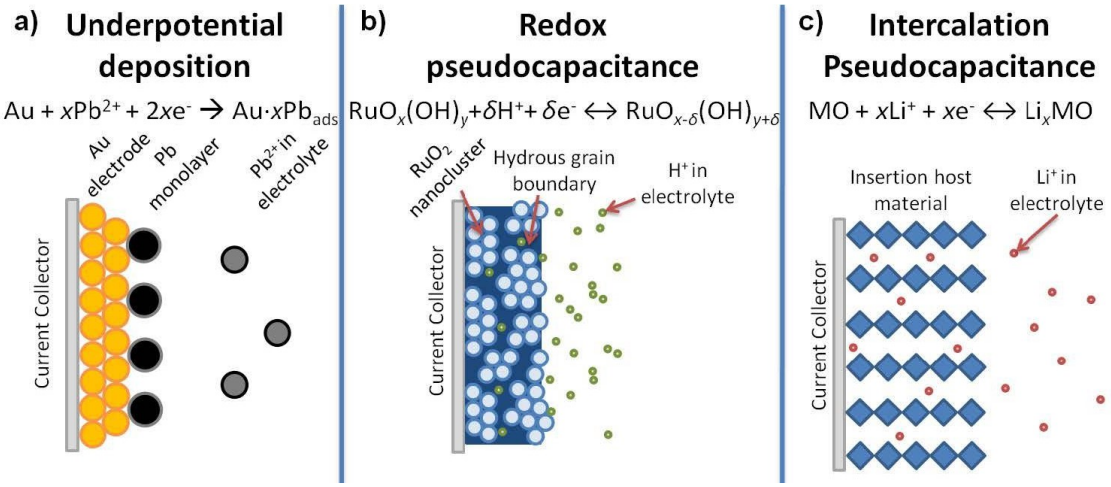

Figure 1.22: Schematic of pseudocapacitive systems identified by Conway.[80] (Figure is taken from open access internet source)

1.5.8 Charge Storage mechanism in Pseudocapacitors

From a thermodynamic perspective, pseudocapacitance can be associated with potential by Equation 1.15, where α is a system property that is directly proportional to the amount of charge transferred. [75]

$$\frac{\alpha}{1-\alpha} = \mathrm{K}\, e^{\frac{VF}{RT}} \qquad (1.15)$$

The accumulation of charge in the under-potential deposition system happens through the potential-dependent adsorption of ad-atoms (H, Pb, Cu) onto the metal surface (Pt, Au, Ag). For the H-Pt system, this process involves two-dimensional surface reactions that adhere to the Langmuir isotherm. As a result, Equation 1.16 can be reformulated as Equation 1.15.

In this equation, θ_H is the coverage fraction of the surface with H on Pt, and CH^+ is the concentration of H^+ ions.

$$\frac{\theta_H}{1-\theta_H} = \mathrm{K}C_H + e^{\frac{VF}{RT}} \qquad (1.16)$$

This equation gives a range of potential that corresponds to a range of θ_H. The capacitance is defined by Equation 1.17.

$$C_\phi = q_H \frac{d\theta_H}{dV} = \frac{qH^F}{RT}\theta_H(1-\theta_H) \qquad (1.17)$$

From Equation 1.17, the highest value of capacitance, $\frac{qH^F}{RT}$, is realized at $\theta_H = 0.5$. Substituting qH approximately to be 210 μC cm^{-2}, the maximum capacitance value reachable for the H-Pt system is about 2200 μF cm^{-2}.[75] In any case, the use of the Langmuir isotherm for its determination implies no interaction between adatoms and metals; in contrast, Boudart chemisorption would modify the surface electron distribution.[71] Based on this observation, Conway and Gileadi suggested an adsorption isotherm incorporating an interaction energy term, gθ, to incorporate such interactions.

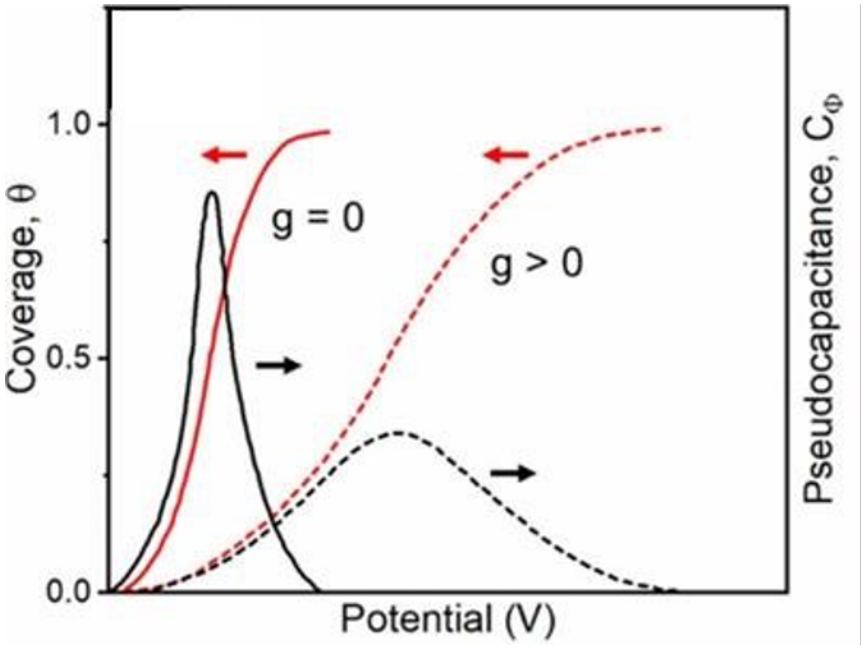

Figure 1.23: shows the variation of pseudocapacitance, Cφ, and surface coverage, Θ, for ideal Langmuir electrosorption (g=0) and Frumkin electrosorption (g>0) [75][82].

The Eq.1.17 can be modified to Eq.1.18 where maximum capacitance is achieved when θ_H=0.5,

$$C_\phi = \frac{qH^F}{RT}\frac{\theta_H(1-\theta_H)}{1+g\theta_H(1-\theta_H)} \qquad (1.18)$$

Despite the large pseudocapacitance associated with underpotential deposition, the high cost of substrates made from noble metals has limited their applications.[78] Nevertheless, the

principles of chemisorption and interaction energy can be applied to redox and intercalation pseudocapacitance systems. In the case of redox pseudocapacitance, ions are electrochemically adsorbed on the surface of active materials, and faradic charge transfer occurs in the process.[80] Typical redox pseudocapacitors are made of metal oxides and conducting polymers and ion adsorption for both of these materials is usually favored by charge compensation.

A general redox reaction is expressed by:

$$Ox + ne^{-} \rightarrow Red. \qquad (1.19)$$

For such a system, the Nernst equation can be applied which is given as:

$$E = E^{0} + \frac{RT}{nF} \ln \frac{[O_x]}{[O_x]+[Red]} \qquad (1.20)$$

By manipulating the Nernst equation, Eq. 1.19 can be brought into a form analogous to Eq. 1.15, but this time in terms of the extent of redox reactions. Again, one finds a similar conclusion, namely that the potentials are logarithmically related to the extent of the reactions. This potential dependence was demonstrated by Toupin et al. on MnO_2 thin and thick film electrodes, using X-ray photoelectron spectroscopy (XPS), and showed that the oxidation state of MnO_2 in thin-film electrodes depends on the potential.[83] Another important observation made by Toupin et al. was that the oxidation state of MnO_2 in thick films does not change with potential, indicating that the charge storage mechanism in this case was similar to that of carbon electrodes, where only a thin layer of MnO_2 is electrochemically active. [83]

$$\frac{[O_x]}{[O_x]+[Red]} = e^{\frac{\Delta EnF}{RT}} \qquad (1.21)$$

Intercalation Pseudocapacitance also involves redox reactions, as ions intercalate into the

tunnels or layers of active materials, accompanied by faradaic charge transfer, but without a crystallographic phase change. These reactions occur in a 3-dimensional structure, not like the 2-dimensional surface that is involved in redox Pseudocapacitance. As with underpotential deposition and redox Pseudocapacitance, the extent of intercalation can be correlated to a range of potential as demonstrated in Eq. 1.22, where X stands for the fraction of ionic occupancy in the lattices.

$$\frac{X}{1+X} = e^{\frac{\Delta EnF}{RT}} \qquad (1.22)$$

Costentin and Saveant performed an electrochemical investigation to identify the source of pseudocapacitance using MnO_2 and hydrous RuO_2 electrodes. Active centers in these materials lie close to the metal-oxide surface, with distances smaller than $<<(2Dt)^{1/2}$, where D is the diffusion coefficient for charge-compensating ions, and t is the diffusion time (s) [84]. These studies have established that electrochemical behavior in these materials is due to the electric double layer (EDL) formed on the conductive surface or a combination of surface Faradaic and EDL processes.

1.5.9 Electrochemical features of pseudocapacitors

Cyclic voltammetry is extensively used in order to investigate pseudocapacitance by observing the "mirror image" feature and the response between current and sweep rate. The pseudo-linearity and hysteresis witnessed in galvanostatic discharge curves also point towards being a material with pseudocapacitance properties. EIS helps with assessing the pseudocapacitive behavior by seeing into the real and imaginary impedance, capacitance and the phase angle. Typical material cyclic voltammograms and galvanostatic discharge curves can be seen in **Figure 1.24**. In this classification, Type B pseudocapacitance is Faradaic, whereas Type C Faradaic does not exhibit capacitive behavior.

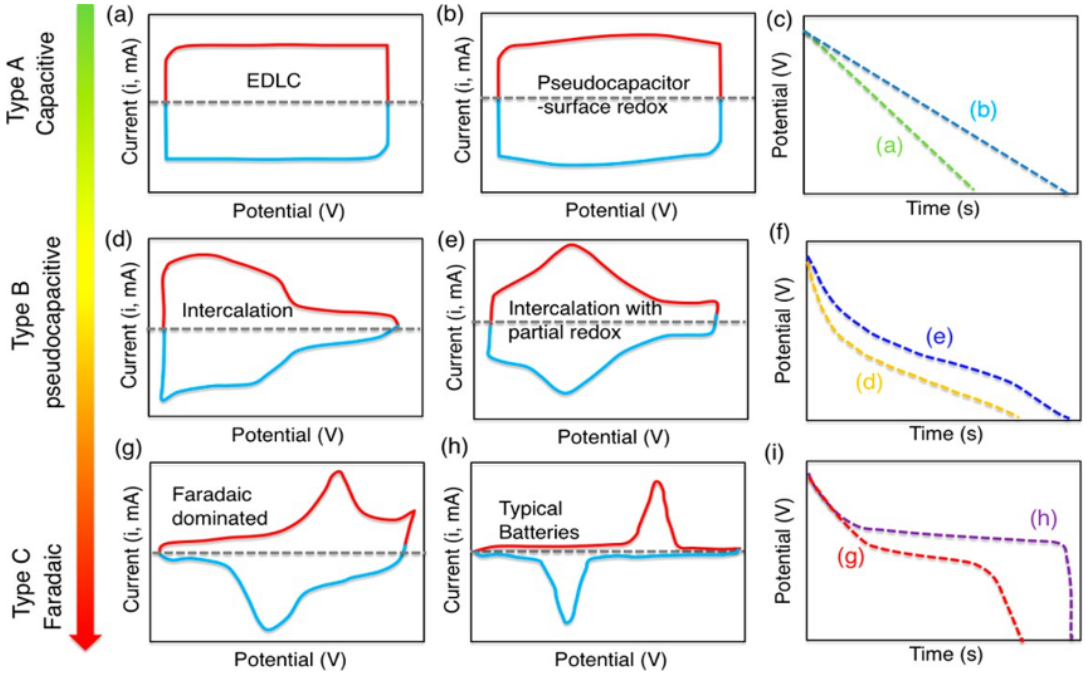

Figure 1.24: Schematic cyclic voltammograms (a,b,d,e,g,h) and corresponding galvanostatic profiles (c,f,i) of various types of charge storage systems [84]

1.6 Electrode Materials

Transition metal oxides and hydroxides are well recognized as excellent materials for pseudocapacitors due to their capability to retain multiple stable oxidation states and their high theoretical capacitance. The faradic surface reactions of these materials occur very rapidly, resulting in higher energy densities than EDLCs. A number of metal oxides and hydroxides such as RuO_2, MnO_2, V_2O_5, NiO, Co_3O_4, Fe_2O_3, and FeOOH have been widely studied for energy storage systems (ESs). However, most of these metal oxides have some drawbacks such as low electrical conductivity and limited participation in irreversible redox reactions.

These issues can be overcome by integrating conductive carbon materials into the fabrication process to form composite electrodes.[68], [85] A summary of the various types of electrodes developed to date is shown below:

1.6.1 Ruthenium dioxide (RuO_2)

Ruthenium dioxide (RuO_2) was among the first metal oxides investigated for application in energy storage systems (ESs). Both crystalline and amorphous hydrous forms have the desirable properties of faradic active materials, such as multiple oxidation states, excellent electrical and ionic conductivity, and strong cyclic stability.[85] In 1971, Trasatti et al. prepared RuO_2 thin films through thermal decomposition, which showed a capacitive response in 1M $HClO_4$ electrolyte with an operating potential range between 0 and 1.45V vs RHE. [86] Charge storage process of RuO_2 in acidic conditions is expressed by:

$$RuO_2 + xH^+ + xe^- \leftrightarrow RuO_{2-}(OH)_x \qquad (1.23)$$

The pseudocapacitance of RuO_2 thin films is attributed to sequential redox transitions of Ru^{2+} to Ru^{4+} and the transformation of OH^- into O^{2-} through proton transfer.[85] Charge transfer and diffusion processes, including electron hopping within and between RuO_2 particles, electron movement from active materials to current collectors, and ion diffusion through RuO_2, determine the efficiency of RuO_2 electrodes.[87]

Among its two phases, the hydrous RuO_2 shows greater capacitance than the anhydrous phase. Sugimoto et al. investigated capacitive performance of RuO_2 with different water contents and showed that the anhydrous RuO_2 has substantially lower capacitance (24 F g^{-1}) than the hydrous counterpart (342 F g^{-1}).[88] They assigned this to the "tree root model," where anhydrous RuO_2 particles are agglomerated and do not have the micropores for diffusion of ions. Hydrous RuO_2 has smaller particles with hydrated micropores that facilitate effective ion transport. Therefore, the water content in RuO_2 is essential for allowing fast ionic conduction through its porous structure, thus enhancing the overall capacitive performance.[88]

Although RuO_2 exhibits ideal properties for applications in energy storage systems (ESs), it has been too expensive for extensive use. To remove the limitation, researchers have searched

for ways to prepare low-cost RuO_2 composites with low-cost metal oxides or to deposit RuO_2 onto conductive substrates.[89] For example, Hu et al. have synthesized a hydrous RuO_2-TiO_2 nanocomposite through a hydrothermal process with a very good capacitance of 992 F g^{-1} at a scan rate of 100 mV s^{-1}.[90] Analogously, Hsieh et al. prepared a composite of vertically aligned multi-walled carbon nanotubes (MWCNTs) coated with hydrous RuO_2 on a titanium current collector and reported a maximum capacitance of 1652 F g^{-1} .[91]

1.6.2 Manganese dioxide (MnO_2)

MnO_2 has been a widely studied candidate for energy storage applications because of its high theoretical capacitance, 1370 F g^{-1}, low cost, low toxicity compared to other metal oxides, and presence of multiple oxidation states.[92],[89] Similar to RuO_2, the pseudocapacitance of MnO_2 stems from the redox transition between Mn^{3+} and Mn^{4+},[68] and the charge storage process is given by Eq. 1.24.

$$MnO_2 + H_2O + e^- \rightarrow MnOOH + OH^- \qquad (1.24)$$

One of the most important benefits of using MnO_2 over RuO_2 is its ability to operate in more mild aqueous electrolytes, including Na_2SO_4 and chloride salts (KCl, NaCl), compared to the strong acids or bases needed by RuO_2-based systems.[85] This gives MnO_2 a lot of versatility and practicality in many energy storage facilities.

MnO_2 exists in different crystal structures, and that includes α, β, γ, δ, and λ phases, each containing its own tunnel structure so the electrolyte can come through to the material. Tunnels in each phase range from 1.89 to 7 Å;[93] the size of the tunnel thus affects electrochemical behaviour. Brousse et al. and Devaraj et al. studied the capacitance of various MnO_2 structures in 0.1 M K_2SO_4 and 0.1 M Na_2SO_4 solutions, respectively. Both of them concluded that the capacitance decreases in the order $\alpha \cong \delta > \gamma > \lambda > \beta$.[93][94]

Another important investigation was that of the surface areas of various MnO_2 structures by Ghodbane et al., with a view to identifying a correlation between surface area and capacitance. From these studies, it seems that the capacitance is much more sensitive to ionic conductivity than to the BET surface area,[95] showing the contribution of ion intercalation into the bulk of MnO_2 to the charge storage mechanism. The properties, crystal structures, and charge storage mechanisms of MnO_2 thus show a material that can be used as an efficient energy storage material, having performance, cost, and adaptability balanced in electrochemical applications.[94], [95]

Despite its good theoretical capacitance and electrolyte compatibility in aqueous electrolytes, one major drawback of MnO_2 is its poor electrical conductivity.[89],[92] The electrical conductivity of electrode materials greatly influences capacitance and rate performance. As the charge-discharge rate increases, low conductivity by electrode materials restricts charge storage in a confined volume and gives a reduced capacitance with poor rate performance.

1.6.3 Vanadium pentoxide (V_2O_5)

V_2O_5 has shown great promise as an active material for batteries and energy storage systems (ESs), in addition to manganese oxides. It provides several advantages, including high energy density, low toxicity, cost-effectiveness, a stable layered structure, and a wide potential window because of its multiple oxidation states between V^{2+} and V^{5+}.[69], [79], [87], [96]

Lee and Goodenough were the first to prepare an amorphous $V_2O_5 \cdot nH_2O$ composite electrode. They obtained this by quenching V_2O_5 powder heated to 1223 K for 30 minutes in deionized water, then ball-milling it with acetylene black and polytetrafluoroethylene (PTFE), before pressing it onto a titanium substrate[67]. Their results showed a near mirror-image cyclic voltammogram between -0.2 and 0.8 V vs. SCE in a 2M KCl electrolyte at a low pH of 2.32, which indicated the pseudocapacitance properties of amorphous V_2O_5. The specific

capacitance was 346.4 F g^{-1}.[97] However, they found that the V_2O_5 composite electrode dissolved at -0.1 V vs. SCE in a 2M KCl electrolyte with a pH of 6.67. This dissolution problem could be overcome by moving the electrolyte to a more acidic condition. Furthermore, V_2O_5 suffers from the same problem of low electrical conductivity as MnO_2. Zhu et al. synthesized a 3D network of V_2O_5 nanosheets, this approach was synthesis of 2D nanosheets by hydrothermal process followed by freeze-drying. The porous 3D structure gave a high specific capacitance of 451 F g^{-1} in a neutral Na_2SO_4 electrolyte and retained more than 90% capacitance after 4000 cycles.[98]

Qu et al. have taken a different approach: they improved conductivity and diminished dissolution by incorporating a core-shell structure. They have coated V_2O_5 nanoribbons with polypyrrole (PPy). This electrode showed an impressive specific capacitance of 308 F g^{-1} in 0.5 M K_2SO_4 electrolyte. After 10,000 cycles, the electrode maintained less than 5% of its capacitance; pure V_2O_5 lost 17.5% under similar conditions.[99]

1.6.4 Nickel oxide (NiO) & nickel hydroxide ($Ni(OH)_2$)

NiO is a very promising material for ESs applications due to its very high theoretical capacitance of 2584 F g^{-1}, affordability, and low toxicity.[100],[101] NiO is usually synthesized by first forming $Ni(OH)_2$, which is then annealed at high temperatures to produce NiO. [87]

Typically, NiO electrodes function in alkaline electrolytes. The charge storage mechanism is still not clear in detail. Two theories are proposed to explain the pseudocapacitance of NiO in these solutions, the first theory is redox reactions between NiO and nickel oxyhydroxide (NiOOH) (Eq.1.24 to Eq. 1.25),[88] and the latter theory involves reactions between $Ni(OH)_2$ and NiOOH (Eq.1.26 & 1.27). However, it is commonly believed that Eq.1.26 occurred first to produce NiOOH, followed by the reversible redox reactions between $Ni(OH)_2$ and NiOOH[71].

$$NiO + OH^{-} + \leftrightarrow NiOOH + e^{-} \quad (1.25)$$

$$NiO + H_2O + e^{-} \leftrightarrow NiOOH + H^{+} + e^{-} \quad (1.26)$$

$$N(OH)_2 \leftrightarrow NiOOH + H^{+} + e^{-} \quad (1.27)$$

$$N(OH)_2 + OH^{-} \leftrightarrow NiOOH + H_2O + e^{-} \quad (1.28)$$

NiO has several drawbacks, such as an achievable specific capacitance that is much lower than its theoretical value, low electrical conductivity, and poor cyclic stability.[89] Similar to other metal oxides, the nanostructured NiO or NiO composites with other materials have been focused on in order to overcome these drawbacks.[101]-[105] Nam et al. studied the electrochemical performance of porous NiO films derived from electroplated $Ni(OH)_2$ films on nickel foil substrates. The films prepared in this study were deposited by various current densities and then heat treated. According to the results, specific capacitance of the NiO film increases with the rate of deposition. A specific capacitance as high as 277 F g^{-1} in the case of 1M KOH electrolyte was reported when deposited at a current density of 4 mA cm^{-2}. [101] Yuan et al. further researched the improvement in NiO performance by designing porous nano- and microspheres through a low temperature precipitation reaction by using alkaline solutions and nickel salts. Their work resulted in an electrode that showed 525 F g^{-1} at a current density of 4 A g^{-1}. The hierarchical porosity contributed by the nano- and microspheres also resulted in excellent capacitance retention, which was reported to be 98% even after 2000 cycles.[106]

$Ni(OH)_2$ has a hexagonal layered structure with two polymorphs, α-$Ni(OH)_2$ and β-$Ni(OH)_2$, and it has been shown that the structure affects the electrode performance.[107] The structure of α-$Ni(OH)_2$ is intercalated with anions and water, while β-$Ni(OH)_2$ lacks water.[107] The α-$Ni(OH)_2$ presented higher specific capacitance than β-$Ni(OH)_2$, and the situation can be

explained by recalling that hydrous RuO_2 showed higher specific capacitance than the anhydrous form due to improved ion transport.[88], [108], [109]

1.6.5 Cobalt oxide (Co_3O4) & cobalt hydroxide ($Co(OH)_2$)

Co_3O_4 is an up-and-coming active material in energy storage systems (ESs) due to its theoretical capacitance value of 3560 F g^{-1}, economical price, great corrosion resistance, and a high degree of electrochemical stability.[68],[100] Co_3O_4 electrodes mainly work in alkaline mediums. Charge storage is well-represented by the reaction below (Eq. 1.29):

$$Co_3O_4 + H_2O + OH^- \leftrightarrow 3CoOOH + e^- \qquad (1.29)$$

Despite its potential, the actual capacitance of Co_3O_4 is much lower than its theoretical value, primarily due to poor conductivity.[110] Nanostructured Co_3O_4 has been fabricated such as nanotubes[110], nanosheets[111], nanotubes[112], nanowire arrays[113], and composite with graphene[114] and porous carbon[112] were also investigated. Salunkle et al. synthesized nanoporous Co_3O_4 using a metal-organic framework. The nanoporous structure allowed a large surface area for charge storage, and the electrode exhibited a specific capacitance of 504 F g^{-1} at a scan rate of 5 mV s^{-1} in a 6M KOH electrolyte. [112] Interestingly, cyclic stability tests showed that the specific capacitance increased to around 1100 F g^{-1} after 500 cycles, after which it remained constant. [114] The authors attributed this behavior to an activation process that enhanced intercalation and deintercalation during charge-discharge cycles. $Co(OH)_2$ also has attracted much attention because it has a layered structure with wide spacings, which allows rapid ion transport during intercalation and deintercalation.[89]

$Co(OH)_2$ however has a narrow potential window of about 0.5 V to sustain its hydroxide structure.[114], [115] Kong et al. prepared an Asymmetric Supercapacitor using α-$Co(OH)_2$ and activated carbon (AC). The α-$Co(OH)_2$ electrode was shown to have the exceptional specific

capacitance as 735 F g^{-1} in 0 to 0.4 V versus SCE, and it demonstrated a specific capacitance as high as 72.4 F g^{-1} within a window from 0 to 1.6 V.[115] Jagadale et al. investigated the electrochemical characteristics of β-$Co(OH)_2$ thin layers deposited by potentio dynamic method onto stainless steel substrates. For a potential range of -0.2 to 0.4 V vs. SCE, it reached an outstanding specific capacitance of 890 F g^{-1} in the 1M KOH solution. [116]

1.6.6 Iron oxide (Fe2O3) & iron hydroxide (FeOOH)

Iron oxides (Fe_2O_3 or Fe_3O_4) have excellent pseudocapacitive charge storage performance because of the rapid and reversible Fe^{2+}/Fe^{3+} redox reactions, high overpotential for the hydrogen evolution reaction (HER), affordability, and high theoretical capacitance. However, their poor conductivity (~10^{-14} S cm^{-1}) and low ionic diffusion rate result in a lower power density. These issues have been overcome by hundreds of iron oxide-based composites, which provide large electrochemically active surface areas and short ion diffusion lengths. For example, Xia et al. produced Fe_2O_3 quantum dots 2 nm in size deposited on functionalized graphene sheets to achieve an excellent specific capacitance of 347 F g^{-1} between -1 to 0 V (vs Ag/AgCl) in a Na_2SO_4 electrolyte. The charge storage mechanism of Fe_2O_3 in an alkaline medium is as follows:

$$\frac{1}{2}Fe_2O_3 + \frac{3}{2}H_2O + e^- \leftrightarrow Fe(OH)_2 + OH^- \qquad (1.30)$$

Liang et al introduced the phosphine plasma activation process to enhance the capacitive performance of the Fe_2O_3 nanorods.[117] Such a dense Fe_2O_3-P electrode attained remarkably high areal capacitance, 340 mF cm^{-2} against the pristine Fe_2O_3, which presented just 66 mF cm^{-2} in the working window of -0.8 to 0 V (vs Ag/AgCl) with a 1 M Na_2SO_4 solution as an electrolyte.

1.6.7 Intercalation Pseudocapacitance in Transition metal oxides

Layered transition metal oxides have excellent charge storage efficiency by the intercalation and deintercalation of ions, and they are, therefore, suitable for high-energy and high-power density applications. Their wide interlayer spacing and weak interlayer bonding allow them to accommodate different guest species, such as cations, anions, and polymers. Furthermore, the ability to tune the solid-state environment in these materials enhances their ability to facilitate multivalent ion intercalation, improve interfacial charge transfer, and support solid-state diffusion.

Intercalation pseudocapacitance results from redox reactions occurring both at the surface and in the bulk, not limited by solid-state diffusion or phase transitions. The general equation for intercalation is expressed as:

$$MA_y + xLi^+ + xe^- \leftrightarrow Li_xMA_y \quad (1.31)$$

In general, the transition metals are in the high oxidation states, that is, +4, +5, and +6. Some examples of transition metal oxides with layered structures follow:

1.6.7.1 Intercalation pseudocapacitance in Nb_2O_5

Intercalation pseudocapacitance is a charging mechanism in which ions are inserted into a layered or tunnel-like structure. While this process makes the potential vary with the degree of ion insertion, it is not generally capacitive due to the limitations of solid-state diffusion kinetics. Most intercalation-based materials are therefore better suited to longer timescales, like hours, and thus make good batteries.

However, the non-aqueous Li^+ electrolyte was used in research on Nb_2O_5 nanocrystals, which showed surprisingly fast charge storage behavior, determined to be capacitive. Later studies established some characteristics that are specific to intercalation pseudocapacitance, such as a crystalline structure that allows for 2D ion transport with minimal structural change during

intercalation, current behavior inversely proportional to time, charge storage capacity largely unaffected by rate, and redox peaks with minor voltage offsets, even at high charge rates.

The major advantage of intercalation pseudocapacitance is that it is able to achieve significant charge storage over short durations, since it avoids the limitations associated with solid-state diffusion.

Intercalation pseudocapacitance and the high-rate performance of Nb_2O_5 was explored using two electrode techniques over a wide range of sweep rates. A thin-film electrode was used for longer timescales, spanning from about 3 hours to 60 seconds (sweep rates of 0.1–20 mV s^{-1} within a 1.2 V voltage window). For shorter timescales where ohmic polarization is prominent (sweep rates: 60–500 mV s^{-1}), a cavity microelectrode was used. To minimize electrical transport losses, that is, ohmic losses, the active material was blended with conductive carbon black.[118]

The study suggests that Nb_2O_5 shows pseudocapacitive electrochemical behaviour despite the fact that charge storage occurs in the bulk material. This is compatible with intercalation pseudocapacitance. Essential features of this mechanism include currents increasing linearly with sweep rate, capacity staying relatively insensitive to charging time, and peak potentials not strongly dependent on changes in sweep rate.

A good atomic-scale design for intercalation pseudocapacitance is a structure that does not exhibit phase transitions during intercalation. Efficient 2D pathways for lithium-ion diffusion are also important. Charge storage processes with quasi-2D behavior are similar to those for 2D surface adsorption reactions.[78] Pseudocapacitive $RuO_2 \cdot xH_2O$ stores charge almost entirely on or very near its surface.[80][119],[120]

1.7 Types and behaviours of Electrochemical pseudocapacitive cells

A Supercapacitor typically consists of a positive electrode, known as the cathode, and a negative electrode, known as the anode, immersed in an electrolyte, separated by an ion-permeable membrane. Electrolytes can be aqueous or non-aqueous, and each type only operates effectively within a specific potential range. Thus, researchers are always working on developing electrode materials that hold electrochemical performance stably within distinct windows to create high-voltage Supercapacitors. The working window of the device is actually determined by the standard electrode potentials of both the positive and negative electrodes connected with their Fermi energies (ƐF).[121] **Figure 1.25** shows the standard electrode potentials for commonly used electrodes in relation to the electrolyte.

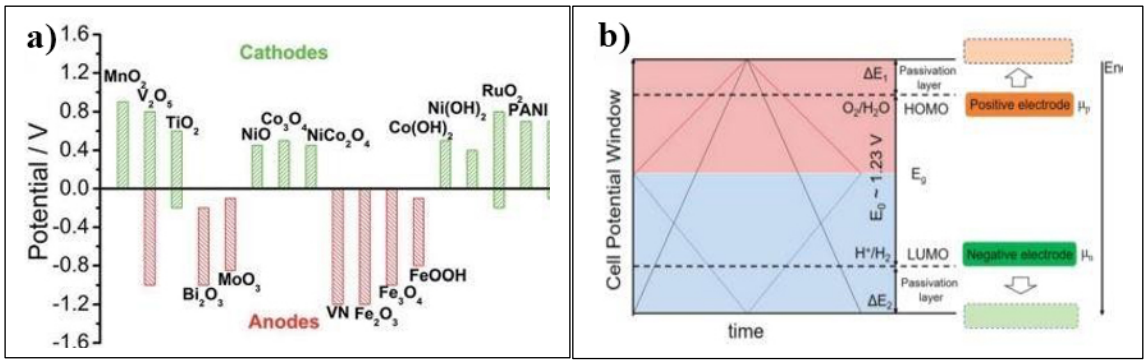

Figure 1.25: (a) Standard electrode potential of some common widely used electrodes, and (b) cell voltage of an aqueous system along with electron energies of active materials [122].

The operating voltage of the Supercapacitor depends on three main factors: electrolyte's stable potential window, the standard potential of each electrode, and formation of a passivation layer at the electrode/electrolyte interface. Theoretically, potential window of the Supercapacitor can be determined as: [123]

$$E_{device} = E_{positive} - E_{negative} \qquad (1.32)$$

Furthermore, based on the standard electrode potential of an electrode, the potential window of the Supercapacitor can be calculated using the following equation:[124]

$$E_{device} = E_0 + \Delta E_1 + \Delta E_2 = \frac{(\omega^{\alpha} - \omega^{\beta})N_A}{F} + \Delta E_1 + \Delta E_2 \quad (1.33)$$

Where ΔE_1 and ΔE_2 are the working potential windows of the positive and negative electrodes in a three-electrode system, and ω^{α} & ω^{β} represent the work functions of the positive and negative electrodes, respectively. In the last few decades, several types of devices have been proposed to enhance the energy density of Supercapacitors.[125][126] These devices can be classified into four basic configurations: type I, which uses symmetric electrodes based on Electric Double-Layer Capacitors (EDLC); type II, which uses symmetric electrodes based on pseudocapacitive materials; type III, which combines EDLC and pseudocapacitive electrodes in an Asymmetric arrangement; and type IV, which consists of Asymmetric electrodes with two different pseudocapacitive materials.

1.7.1 Symmetric Cell

A traditional symmetric Supercapacitor device is formed by using the same type of material for both electrodes with an equal mass loading and it usually only spans a small potential range. As examples, symmetric Supercapacitors using graphene as the electrode material and exhibit an EDLC-type CV with a rectangular shape whereas ones that make use of graphene oxide with pseudocapacitive-type material exhibit quasi-rectangular CV curve.[127] The fundamental electrochemical properties of a symmetric device are given in **figure 1.26**.

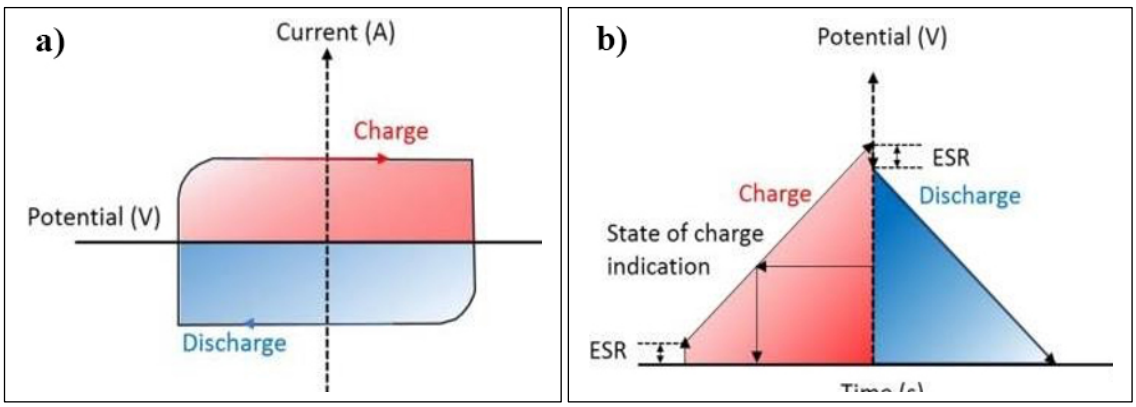

Figure 1.26: CV and GCD curves of symmetrical EDLC- types of electrodes.

1.7.2 Asymmetric Cell

The main objective of designing an Asymmetric configuration is to increase the energy density of a Supercapacitor by increasing its operational potential window. Tang et al. have synthesized Fe_2O_3 nanowires and NiO nanoflakes on carbon fibre paper (CFP) as the negative and positive electrodes, respectively. The fabricated Asymmetric device had a high energy density of 105 Wh/kg at a power density of 1400 W/kg and maintained 72.6 Wh/kg even at 12700 W/kg, outperforming earlier reported Asymmetric Supercapacitors (ASCs).[122] Thus, the Asymmetric Supercapacitor concept is seen as a potential solution to the limitations of narrow potential windows and lower energy density in Supercapacitor devices.

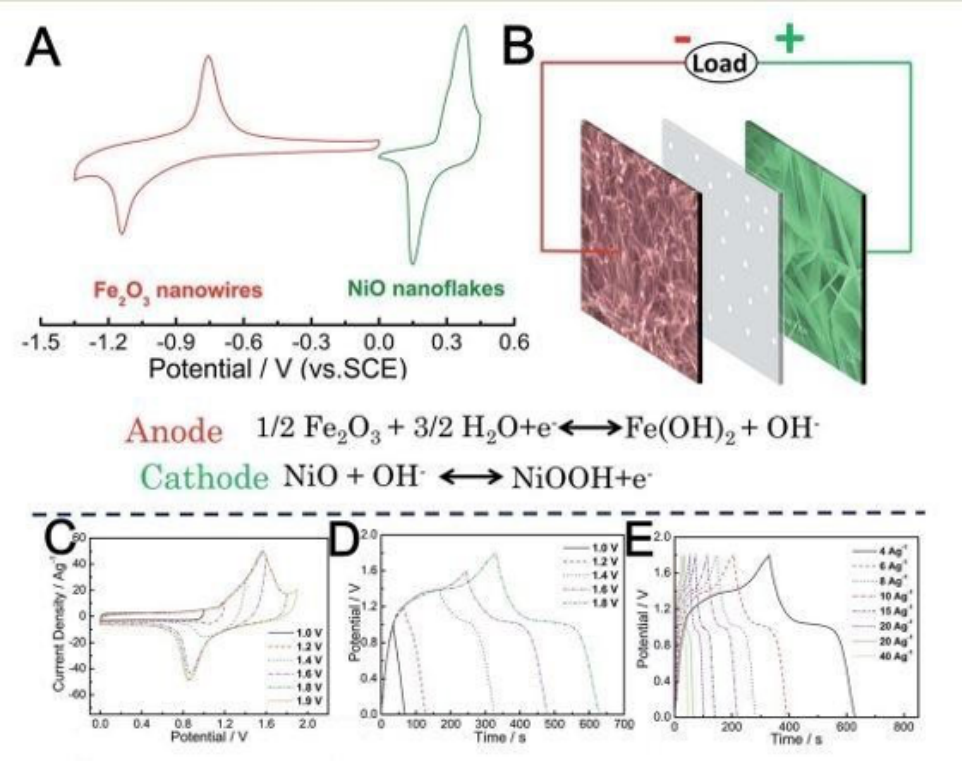

Figure 1.27: Electrochemical features of NiO ‖ Fe_2O_3 device in 6M KOH electrolyte [122]

1.7.3 Hybrid Cell

A Hybrid capacitor is a system where the two electrodes utilize different charge-storage mechanisms: one being capacitive and the other Faradaic, just like a battery. For example, devices featuring a Faradaic electrode, such as $Ni(OH)_2$, and a carbon electrode are examples of Hybrid Capacitor devices.[128] Although one of the electrodes acts as a battery electrode, the CV and GCD curves of the full device may exhibit behavior more capacitive than perfect capacitive characteristics. The energy density of a Hybrid capacitor, with its nonlinear GCD curve, can be calculated using Eq. 1.22:

$$E = \int Q\, dV = \int_{t1}^{t2} IV_{(t)}\, dt \qquad (1.34)$$

Where, t_1 represents the time after initial iR drop, t_2 is the time at which discharged is finished, and I is the constant current applied to the Supercapacitor.

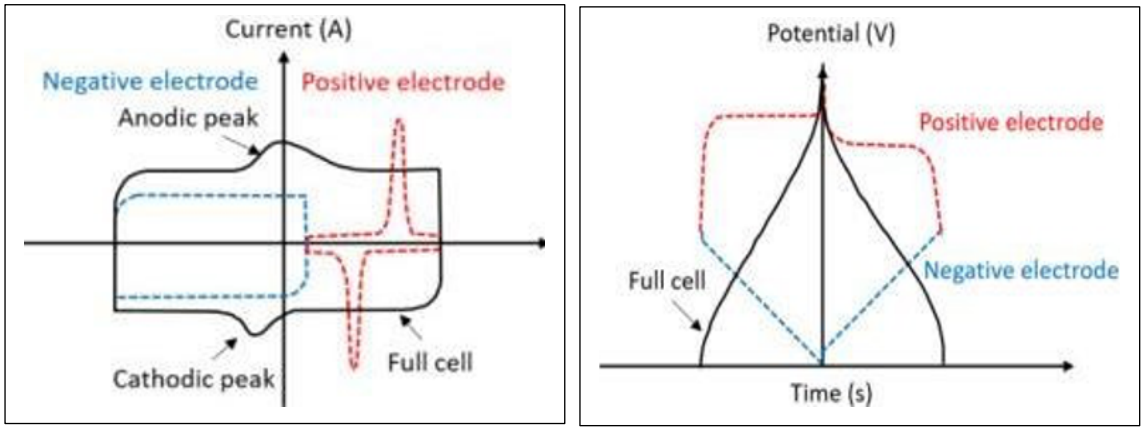

Figure 1.28: Schematic illustration of Hybrid capacitor [128]

1.8 Aim of the Thesis

This thesis aims to establish a link between the crystal structure and electronic properties of materials for the development of high-performance Pseudocapacitor electrodes. Layered transition metal oxides with open-channel structures are promising candidates because they can easily enable rapid diffusion of ions within the framework, delivering high energy density and

power capabilities. The redox energy of these materials is thus influenced by their local electronic structure through metal-ligand bond formation. Therefore, doping with controlled dopant concentration can be used to efficiently vary the crystal structure and the energy bands.

Optimizing electrode material, electrolytes, and a current collector are the purposes of designing aqueous based Asymmetric Supercapacitor devices (AASCs) and Hybrid Supercapacitors (HSCs) , which can have wide working voltage ranges for achieving either high energy and power densities. The kinetic study related to electrochemical reactions from the electrode/electrolyte interfaces is highly focused in the thesis by providing useful knowledge for efficient cell design and electrode development for grid- scale energy storage solution.

References:

[1] Kostic M., Work, Power, and Energy, Elsivier Inc., DeKalb, Illinois, US 2004.

[2] M. Kostic, Proceedings of IMECE2004 2004, 1.

[3] E.U. Information Adminstration - Department Of Energy, Annual Energy Review 2004, 2004.

[4] M. Assumptions Nasir Khilji, International Energy Outlook 2005, 2025.

[5] A. Fawzi, B. Bawks, International Energy Outlook 2002, Washington 2003.

[6] E. Sánchez, Annual Energy Outlook Forecast Evaluation, n.d.

[7] T. Wernberg, B.D. Russell, M.S. Thomsen, S.D. Connell, in Global Environmental Change, Springer Netherlands2014, 181.

[8] I. Renewable Energy Agency, Global Energy Transformation: A Roadmap to 2050, 2018.

[9] D. Gielen, F. Boshell, D. Saygin, M.D. Bazilian, N. Wagner, R. Gorini, Energy Strategy Reviews 2019, 24, 38.

[10] P.A. Owusu, S. Asumadu-Sarkodie, Cogent Eng 2016, 3.

[11] United nation climate action https://www.un.org/en/climatechange/what-is- renewable-energy

[12] Hydrothermal energy https://www.scientist-next-door.org/articles/water-a-source-of-life-and-renewable-energy

[13] United nation climate action https://www.un.org/en/climatechange/what-is- renewable-energy

[14] Modeling and Analysis of Maximum Power Tracking of a 600 kW Hydraulic Energy Storage Wind Turbine Test Rig, www.mdpi.com/journal/processes 2019, 7, 706

[15] Esd solar energy https://esdsolar.com/how-does-solar-energy-work/

[16] Strategic Priorities of Sustainable Energy Development, Sustainable Energy Management, 2013

[17] Geothermal energy https://www.bakerhughes.com/panametrics/success-stories/steam-flow-measurement-geothermal-power-plant

[18] Bioenergy https://cfdflowengineering.com/biomass-waste-incineration-boiler-and-its-applications/

[19] Kazuya Kubo, Yoshinori Kawaharazaki, Hideaki Itoh. Development of large MH tank system for renewable energy storage. International journal of hydrogen energy; 2017, 4, 22475 – 22479.

[20] Pascal Dubucq, Prof.Dr.-Ing.Guunter Ackermann. Optimal Use of Energy Storage Potentials in a Renewable Energy System with District Heating. Energy Procedia; 2017, 135:158 -171.

[21] U. Energy Information Administration, Monthly Energy Review – April 2021, 2021.

[22] K. Handayani, Y. Krozer, T. Filatova, Energy Policy 2019, 127, 134.

[23] K. Kubo, Y. Kawaharazaki, H. Itoh, Int J Hydrogen Energy 2017, 42, 22475

[24] P. Dubucq, G. Ackermann, in Energy Procedia, Elsevier Ltd2017, 158.

[25] Mustafa E. Amiryar and Keith R. Pullen. A Review of Flywheel Energy Storage System Technologies and Their Applications. Applied Sciences 2017.

[26] Electrical Funda Blog. Flywheel as Energy Storage Device, Calculations and Rotor Requirements.http://electricalfundablog.com/flywheel-energy-storage-calculations-rotor.

[27] IEA-ETSAP and IRENA. Thermal Energy Storage Technology Brief E17, 2013

[28] Satyawan Singh, Pradeep Kumar Sharma, Neeru Goyal, Prashant KumarTayal. Thermal Energy Storage: A Process To Increase Efficiency and To Save our Environment. ICLISEM; 2016, 81-87.

[29] Joseph Stekli, Levi Irwin and Ranga Pitchumani. Technical Challenges and Opportunities for Concentrating Solar Power With Thermal Energy Storage. Journal of Thermal Science and Engineering Applications ., 2013, 5(2).

[30] Amit Kumar Rohit, Ksh. Priyalakshmi Devi, Saroj Rangnekar. An overview of energy storage and its importance in Indian renewable energy sector. Journal of Energy Storage; 2017, 13:10–23.

[31] Buckles, W. & Hassenzahl, W., 2000. Superconducting Magnetic Energy Storage. IEEE Power Engineering review; 2020, 16: 16–20.

[32] Energy Storage Sense. Superconducting Magnetic Energy Storage. http://energystoragesense.com/superconducting-magnetic-energy-storage-smes/

[33] Xing Luo, Jihong Wang, Mark Dooner, Jonathan Clarke. Overview of current development in electrical energy storage technologies and the application potential in power system operation. Applied Energy; 2015, 137: 511–536.

[34] Diaz-Gonzalez F, Sumper A, Gomis-Bellmunt O, Villafafila,Robles R. A review of energy storage technologies for wind power applications. Renewable Sustanable Energy; 2012,16:2154–71.

[35] Hydrogen Energy Storage: A New Solution To the Renewable Energy Intermittency Problem. http://www.renewableenergyworld.com/articles/2014/07/hydrogen-energy-storage-a-new-solution-to-the-renewable-energy-intermittency-problem.html

[36] S. Chu, A. Majumdar, Nature 2012, 488, 294.

[37] M. Armand, J.M. Tarascon, Nayure 2008, 45.

[38] J.W. Long, T. Brousse, D. Bélanger, J Electrochem Soc 2015, 162, Y3.

[39] A.S. Aricò, P. Bruce, B. Scrosati, J.M. Tarascon, W. Van Schalkwijk, Nat Mater 2005, 4, 366.

[40] P. Simon, Y. Gogotsi, B. Dunn, Materials Science 2014, 343.

[41] S. Fleischmann, J.B. Mitchell, R. Wang, C. Zhan, D.E. Jiang, V. Presser, V. Augustyn, Chem Rev 2020, 120, 6738.

[42] S. Ghosh, S.R. Polaki, A. Macrelli, C.S. Casari, S. Barg, S.M. Jeong, K. Ostrikov, J Phys D Appl Phys 2022, 55.

[43] voltaic pile, https://nationalmaglab.org/tutorials/source/voltaicpile/voltaicpile.html

[44] J.T. Stock, American Chemical Society 1988.

[45] Katsuhiko Naoi and Yuki Nagano, Supercapacitor: Materials, System, Applications 2013, 239.

[46] M.G.-J.Phys.Theor. Appl., undefined 1910, Hal.ScienceMr GouyJ. Phys. Theor. Appl., 1910 • Hal.Science 1910, 9.

[47] D.L. Chapman, The London, Edinburgh, and Dublin Philosophical Magazine and Journal of Science 1913, 25, 475.

[48] O.Z. Stern, Z.Elektrochem. 1924, 30, 508.

[49] D.C. Grahame, Chem Rev 1947, 41, 441.

[50] S. Trasatti, G Buzzanca, J Electroanal Chem Interfacial Electrochem 1971, 29, A1.

[51] B.E. Convoy, Journal of The ElectrochemicalSociety 1991, 138, 1539.

[52] M. Jayalakshmi, K. Balasubramanian, Simple Capacitors to Supercapacitors-An Overview Article in International Journal of Electrochemical Science · November, 2008.

[53] Callister William D., Jr.D.G. Rethwisch, Materials Science and Engineering, Willey2018.

[54] R. Holze, Journal of Solid State Electrochemistry 2013, 17, 2371.

[55] Petr Krivik, Petr Baca. "Electrochemical Energy Storage". Energy Storage-Technologies and Applications , IntechOpen,2013 ,80-100;. doi:10.5772/52222:.

[56] J. B.,Goodenough & Park, K.-S. The Li-ion rechargeable battery: a perspective. Journal of the American Chemical Society, 2013, 135, 1167–1176.

[57] P. Krivik, P. Bac, in Energy Storage - Technologies and Applications, InTech2013.

[58] M.Calabek, K.Micka, P.Baca, A fundamental study of the effects of compression on the performance of lead accumulator plates,. Journal of Power Sources, 2001 95, 97-107.

[59] J.-M., Tarascon & Armand, M. Issues and challenges facing rechargeable lithium batteries. Nature 2001, 414, 359–367.

[60] C.Angus. Vincent, Bruno. Scrosati, 1997, 351.

[61] Zheng, H., Cathode performance as a function of inactive material and void fractions. J. Electrochem. Soc.,2010, 157, A1060–A1066.

[62] Jeong, H.S., Hong, S.C., Lee, S.Y., Effect of microporous structure on thermal

shrinkage and electrochemical performance of Al2O3/poly(vinylidene fluoride-hexafluoropropylene) composite separators for lithium-ion batteries. J. Membr. Sci.,2010, 364, 177–182.

[63] Cong-Ling, H., Jie, W., Miao, Z., Jin-Ming, Y., Jin-Peng, L., Application of adaptive algorithm of solar cell battery charger,Proceedings of the 2004 IEEE international conference on electric utility deregulation, restructuring and power technologies, 2004, 2, 810–813.

[64] Zheng, H., Cathode performance as a function of inactive material and void fractions. J. Electrochem. Soc.,2010, 157, A1060–A1066.

[65] Christensen, J. et al., A critical review of Li/air batteries. J. Electrochem. Soc.,2012, 159, R1–R30.

[66] Tang, Y. et al., Experimental investigation of dynamic performance and transient responses of a kW-class PEM fuel cell stack under various load changes. Appl. Energy, 2010, 87, 1410–1417.

[67] J. Delsing, F. Häggström, Energy Harvesting and Systems 2018, 5, 43.

[68] G. Wang, L. Zhang, J. Zhang, Chem Soc Rev 2012, 41, 797.

[69] P. Sharma, T.S. Bhatti, Energy Convers Manag 2010, 51, 2901.

[70] T. Chen, L. Dai, Materials Today 2013, 16, 272.

[71] B. E. Conway, Electrochemical Supercapacitors: Scientific Fundamentals and Technological Applications. Boston, MA: Springer US, 1999.

[72] B.E. Conway, V. Birss, J. Wojtowicz, The Role and Utilization of Pseudocapacitance for Energy Storage by Supercapacitors, 1997.

[73] H. DENG, Oxygen Reduction at Soft Interfaces, ÉCOLE POLYTECHNIQUE FÉDÉRALE DE LAUSANNE, 2014.

[74] H. Zhang, W. Zhang, J. Cheng, G. Cao, and Y. Yang, “Acetylene black agglomeration

in activated carbon based electrochemical double layer capacitor electrodes," Solid State Ion.,2008, 179,1946–1950.

[75] H. Nakagawa, A. Shudo, K. Miura, J Electrochem Soc 2000, 147, 38.

[76] H. Tamai, M. Kunihiro, M. Morita, H. Yasuda, Journal of Materials Science 2005, 40, 3703.

[77] V.V.N. Obreja, Physica E Low Dimens Syst Nanostruct 2008, 40, 2596.

[78] B. E. Conway, "Transition from 'Supercapacitor to Battery' Behavior in Electrochemical Energy Storage,"J. Electrochem. Soc.,1991, 138 ,1539-1544.

[79] V. Augustyn, P. Simon, B. Dunn, Energy Environ Sci 2014, 7, 1597.

[80] V. Augustyn, P. Simon, and B. Dunn, "Pseudocapacitive oxide materials for high-rate electrochemical energy storage," Energy Environ. Sci.,2014, 7, 1597-1601.

[81] B.E. Conway, H. Angerstein-Kozlowska, Acc Chem Res 1981, 14, 49.

[82] H. Angerstein-Kozlowska, B.E. Conway, W.B.A. Sharp, J Electroanal Chem Interfacial Electrochem 1973, 43, 9.

[83] M. Toupin, T. Brousse, and D. Bélanger, "Charge Storage Mechanism of MnO2 Electrode Used in Aqueous Electrochemical Capacitor," Chem. Mater.,2004,16, 3184–3190.

[84] Y. Gogotsi, R.M. Penner, ACS Nano 2018, 12, 2081.

[85] M. Y. Ho, P. S. Khiew, D. Isa, T. K. Tan, W. S. Chiu, and C. H. Chia, "A review of metal oxide composite electrode materials for electrochemical capacitors," Nano, 2014, 09, 143-149.

[86] Trasatti, S. & Buzzanca, G. Ruthenium dioxide: a new interesting electrode material. Solid state structure and electrochemical behaviour. Electroanalytical chemistry and interfacial electrochemistry, 1971, 29, 1–5.

[87] C. D. Lokhande, D. P. Dubal, and O.-S. Joo, "Metal oxide thin film based

supercapacitors," Curr. Appl. Phys.,2011, 11, 255–270.

[88] W. Sugimoto, H. Iwata, K. Yokoshima, Y. Murakami, and Y. Takasu, "Proton and Electron Conductivity in Hydrous Ruthenium Oxides Evaluated by Electrochemical Impedance Spectroscopy: The Origin of Large Capacitance," J. Phys. Chem. B,2005, 109, 7330–7338.

[89] F. Shi, L. Li, X. Wang, C. Gu, and J. Tu, "Metal oxide/hydroxide-based materials for supercapacitors," RSC Adv, 2014, 4, 41910–41921.

[90] C.-C. Hu, Y.-L. Yang, and T.-C. Lee, "Microwave-Assisted Hydrothermal Synthesis of RuO[sub 2]·xH[sub 2]O–TiO[sub 2] Nanocomposites for High Power Supercapacitors," Electrochem. Solid-State Lett.,2010, 13, 173-185.

[91] T.-F. Hsieh, C.-C. Chuang, W.-J. Chen, J.-H. Huang, W.-T. Chen, and C.-M. Shu, "Hydrous ruthenium dioxide/multi-walled carbon-nanotube/titanium electrodes for supercapacitors," Carbon, 2012, 50,1740–1747.

[92] M. Huang, F. Li, F. Dong, Y. X. Zhang, and L. L. Zhang, "MnO2 -based nanostructures for high-performance supercapacitors," J. Mater. Chem. A,2015, 3, 21380–21423.

[93] S. Devaraj and N. Munichandraiah, "Effect of Crystallographic Structure of MnO2 on Its Electrochemical Capacitance Properties," J. Phys. Chem. C,2008, 112, 4406– 4417.

[94] T. Brousse, M. Toupin, R. Dugas, L. Athouël, O. Crosnier, and D. Bélanger, "Crystalline MnO[sub 2] as Possible Alternatives to Amorphous Compounds in Electrochemical Supercapacitors," J. Electrochem. Soc.,2006 vol. 153, no. 12, p. A2171.

[95] O. Ghodbane, J.-L. Pascal, and F. Favier, "Microstructural Effects on Charge-Storage

Properties in MnO2 -Based Electrochemical Supercapacitors," ACS Appl. Mater. Interfaces,2009, 1, 1130–1139.

[96] B. Saravanakumar, K. K. Purushothaman, and G. Muralidharan,"Interconnected V2O5 Nanoporous Network for High-Performance Supercapacitors," ACS Appl. Mater. Interfaces,2012, 4,4484–4490.

[97] H. Y. Lee and J. B. Goodenough, "Ideal Supercapacitor Behavior of Amorphous V2O5·nH2O in Potassium Chloride (KCl) Aqueous Solution," J. Solid State Chem., 1999, 148,81–84.

[98] J. Zhu ., "Building 3D Structures of Vanadium Pentoxide Nanosheets and Application as Electrodes in Supercapacitors," Nano Lett.,2013, 13, 5408–5413.

[99] Q. Qu, Y. Zhu, X. Gao, and Y. Wu, "Core-Shell Structure of Polypyrrole Grown on V2O5 Nanoribbon as High Performance Anode Material for Supercapacitors," Adv. Energy Mater.,2012, 2,950–955.

[100] Y. Wang, J. Guo, T. Wang, J. Shao, D. Wang, and Y.-W. Yang, "Mesoporous Transition Metal Oxides for Supercapacitors," Nanomaterials, 2015,5,1667–1689.

[101] S.-I. Kim, J.-S. Lee, H.-J. Ahn, H.-K. Song, and J.-H. Jang, "Facile Route to an Efficient NiO Supercapacitor with a Three-Dimensional Nanonetwork Morphology," ACS Appl. Mater. Interfaces,2013, 5,1596–1603.

[102] C.-Y. Cao, W. Guo, Z.-M. Cui, W.-G. Song, and W. Cai, "Microwave-assisted gas/liquid interfacial synthesis of flowerlike NiO hollow nanosphere precursors and their application as supercapacitor electrodes," J. Mater. Chem.,2011, 21,3204-3213.

[103] K.-C. Liu and M. A. Anderson, "Porous Nickel Oxide/Nickel Films for Electrochemical Capacitors," J Electrochem Soc, 1996, 143,7-9.

[104] X. Zhang., “Synthesis of porous NiO nanocrystals with controllable surface area and their application as supercapacitor electrodes,” Nano Res.,2010, 3 643–652.

[105] J. W. Lee, T. Ahn, J. H. Kim, J. M. Ko, and J.-D. Kim, “Nanosheets based mesoporous NiO microspherical structures via facile and template-free method for high performance supercapacitors,” Electrochimica Acta, 2011, 56, 4849–4857.

[106] C. Yuan, X. Zhang, L. Su, B. Gao, and L. Shen, “Facile synthesis and self-assembly of hierarchical porous NiO nano/micro spherical superstructures for high performance supercapacitors,” J. Mater. Chem.,2009, 19,5772-5804.

[107] Y. Ren and L. Gao, “From Three-Dimensional Flower-Like α-Ni(OH)2 Nanostructures to Hierarchical Porous NiO Nanoflowers: Microwave-Assisted Fabrication and Supercapacitor Properties: Rapid Communications of the American Ceramic Society,” J. Am. Ceram. Soc.,2010, 93, 3560–3564.

[108] H. Du, L. Jiao, K. Cao, Y. Wang, and H. Yuan, “Polyol-Mediated Synthesis of Mesoporous α-Ni(OH)2 with Enhanced Supercapacitance,” ACS Appl. Mater. Interfaces; 2013, 5,6643–6648.

[109] M. C. Bernard, P. Bernard, M. Keddam, S. Senyarich, and H. Takenouti, “Characterisation of new nickel hydroxides during the transformation of α Ni(OH)2 to β Ni(OH)2 by ageing,” Electrochimica Acta; 1996, 41,91–93.

[110] J. Xu, L. Gao, J. Cao, W. Wang, and Z. Chen, “Preparation and electrochemical capacitance of cobalt oxide (Co3O4) nanotubes as supercapacitor material,” Electrochimica Acta; 2010, 56, 732–736.

[111] S. Xiong, C. Yuan, X. Zhang, B. Xi, and Y. Qian, “Controllable Synthesis of Mesoporous Co3O4 Nanostructures with Tunable Morphology for Application in Supercapacitors,” Chem. - Eur. J., 2009, 15,5320–5326.

[112] R. R. Salunkhe, J. Tang, Y. Kamachi, T. Nakato, J. H. Kim, and Y. Yamauchi,

"Asymmetric Supercapacitors Using 3D Nanoporous Carbon and Cobalt Oxide Electrodes Synthesized from a Single Metal–Organic Framework," ACS Nano;2015, 9,6288–6296.

[113] X.-C. Dong., "3D Graphene–Cobalt Oxide Electrode for High-Performance Supercapacitor and Enzymeless Glucose Detection," ACS Nano, 2012, 6, 3206–3213.

[114] T. Zhao, H. Jiang, and J. Ma, "Surfactant-assisted electrochemical deposition of α-cobalt hydroxide for supercapacitors," J. Power Sources,2011, 196, 860–864.

[115] L.-B. Kong, M. Liu, J.-W. Lang, Y.-C. Luo, and L. Kang, "Asymmetric Supercapacitor Based on Loose-Packed Cobalt Hydroxide Nanoflake Materials and Activated Carbon," J. Electrochem. Soc.; 2009, 156, 1000-1012.

[116] A. D. Jagadale, V. S. Jamadade, S. N. Pusawale, and C. D. Lokhande, "Effect of scan rate on the morphology of potentiodynamically deposited β-Co(OH)2 and corresponding supercapacitive performance," Electrochimica Acta; 2012, 78,92–97.

[117] H. Liang, C. Xia, A.H. Emwas, D.H. Anjum, X. Miao, H.N. Alshareef, Nano Energy 2018, 49, 155.

[118] Come, J., Taberna, P.-L., Hamelet, S., Masquelier, C. & Simon, P. Electrochemical Kinetic Study of LiFePO4 Using Cavity Microelectrode. Journal of The Electrochemical Society 2011, 158,1090–093.

[119] Dmowski, W., Egami, T., Swider-Lyons, K. E., Love, C. T. & Rolison, D. R. Local Atomic Structure and Conduction Mechanism of Nanocrystalline Hydrous RuO2 from X-ray Scattering. The Journal of Physical Chemistry B.,2002, 106, 12677–12683.

[120] Liu, Y., Zhou, F. & Ozolins, V. Ab Initio Study of the Charge-Storage Mechanisms in RuO2 -Based Electrochemical Ultracapacitors. Journal of Physical Chemistry C., 2012, 116, 1450–1457.

[121] F. Wang, X. Wu, X. Yuan, Z. Liu, Y. Zhang, L. Fu, Y. Zhu, Q. Zhou, Y. Wu, W.

Huang, Chem Soc Rev 2017, 46, 6816.

[122] Q. Tang, W. Wang, G. Wang, J Mater Chem A Mater 2015, 3, 6662.

[123] J. Chang, M. Jin, F. Yao, T.H. Kim, V.T. Le, H. Yue, F. Gunes, B. Li, A. Ghosh, S. Xie, Y.H. Lee, Adv Funct Mater 2013, 23, 5074.

[124] W. Qian, F. Sun, Y. Xu, L. Qiu, C. Liu, S. Wang, F. Yan, Energy Environ Sci 2014, 7, 379.

[125] R. Xu, L. Du, D. Adekoya, G. Zhang, S. Zhang, S. Sun, Y. Lei, Adv Energy Mater 2021, 11

[126] J. Yan, Q. Wang, T. Wei, Z. Fan, Adv Energy Mater 2014, 4.

[127] M. Biswal, A. Banerjee, M. Deo, S. Ogale, Energy Environ Sci 2013, 6, 1249.

[128] B. Akinwolemiwa, C. Peng, G.Z. Chen, J Electrochem Soc 2015, 162, A5054